Moisture in the Lower Free Troposphere and Observational Strategies for Obtaining Vertical Profiles In and Near Convection

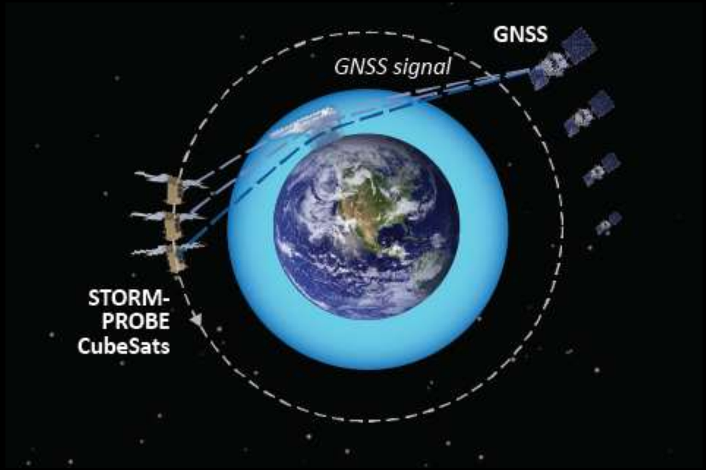

F. Joseph (Joe) Turk

Jet Propulsion Laboratory
California Institute of Technology
Pasadena, CA

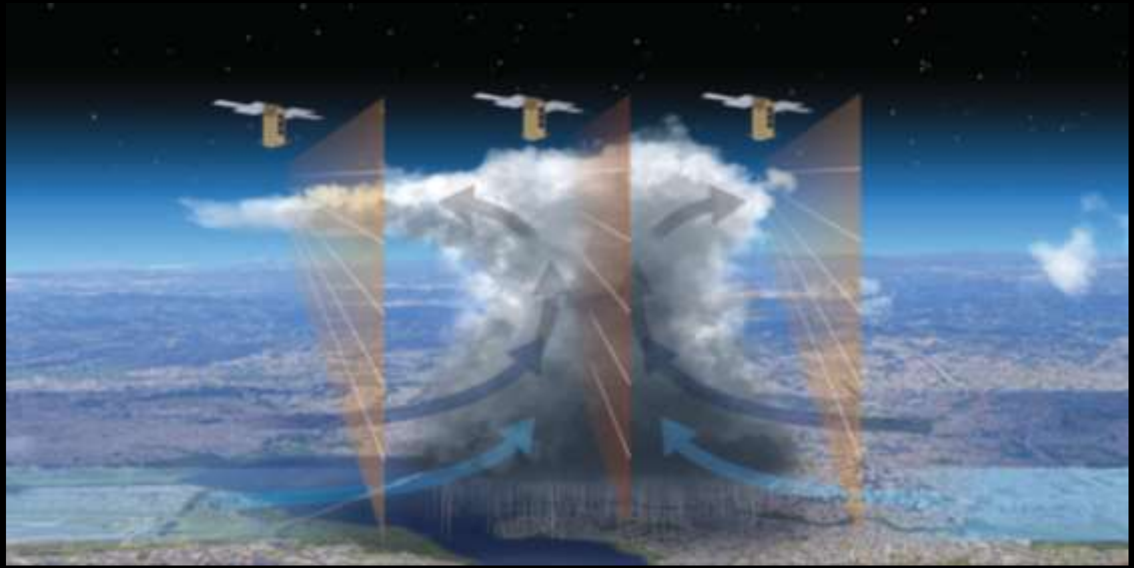

13 April 2023, GESTAR-II Seminar Series

Jet Propulsion Laboratory
California Institute of Technology

Acknowledgements

Manuel de la Torre Juárez, Chi O. Ao, Kuo-Nung Wang, Svetla Hristova-Veleva, Garth Franklin (JPL)

Ramon Padullés, Estel Cardellach (ICE-CSIC, IEEC, Barcelona, Spain)

J. David Neelin, Todd Emmenegger, Fiaz Ahmed (UCLA)

Mayra Oyola-Merced (Univ. of Wisconsin), Yi-Hung Kuo (Princeton/GFDL), Kathleen Schiro (Univ. of Virginia)

Sergio Tomas (Spire, Inc.)

Lidia Cucurull (NOAA/AOML)

About Myself

Originally from Michigan's Upper Peninsula

BS/MS electrical engineering, Michigan Tech, thesis on deep Earth soundings (for siting the Navy's extremely low frequency (ELF) submarine communication system)

Worked for Motorola, Inc in the Chicago area. Production of early cellular mobile telephones (remember the "brick" in the movie "Wall Street" with Michael Douglas?)

PhD Colorado State (Prof. V.N. Bringi, Advisor), use of polarimetric NCAR/CSU radar to estimate precipitation from DMSP/SSMI satellite data, just being released at that time

Naval Research Laboratory, Marine Meteorology Division in 1995 with the group led by Jeff Hawkins, satellite applications, use for NWP, tropical cyclones, post-9/11 support

JPL since 2009, in the "Radar Science" area, interest in passive/active microwave observations for precipitation, evaluating and improving weather and climate models

Moisture and Extreme Precipitation

Extreme precipitation is a key variable for societal impacts in weather forecasting and climate projections. The role of the vertical structure of moisture in the immediate environment of the convection has been identified as a leading factor in controlling extreme events.

Science investigations have been hindered since the measurement of tropospheric water vapor structure in and nearby to heavy precipitation is not routinely observed, or often compromised from traditional IR and MW soundings, especially at lower levels

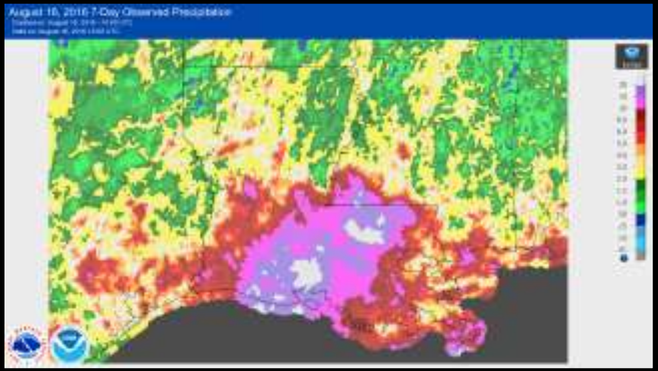

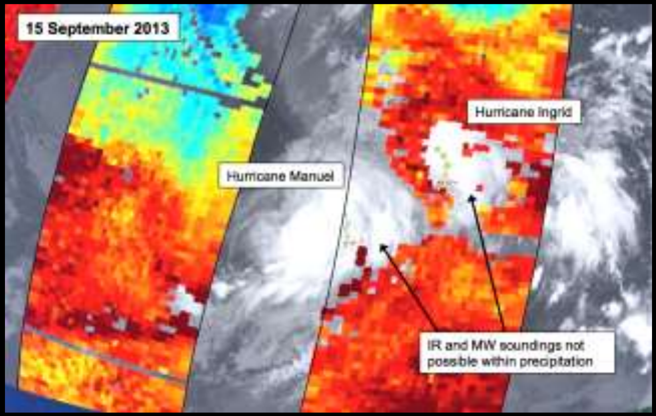

Precipitation-water vapor relation guiding model development

The observed "pickup" of precipitation (P) as a function of layer-averaged water vapor and temperature is captured in models with varying accuracy (Kuo et al., 2018, 2020)

Recent studies point to the role of the lower free troposphere (LFT) moisture, the layer just about the Earth's boundary layer

Convective transition statistics serve as diagnostics for the parameterization of convection in climate and weather forecast models

These characterize the dependence of precipitation on the moisture-temperature environment

Each curve shows the "pickup" from a different climate model

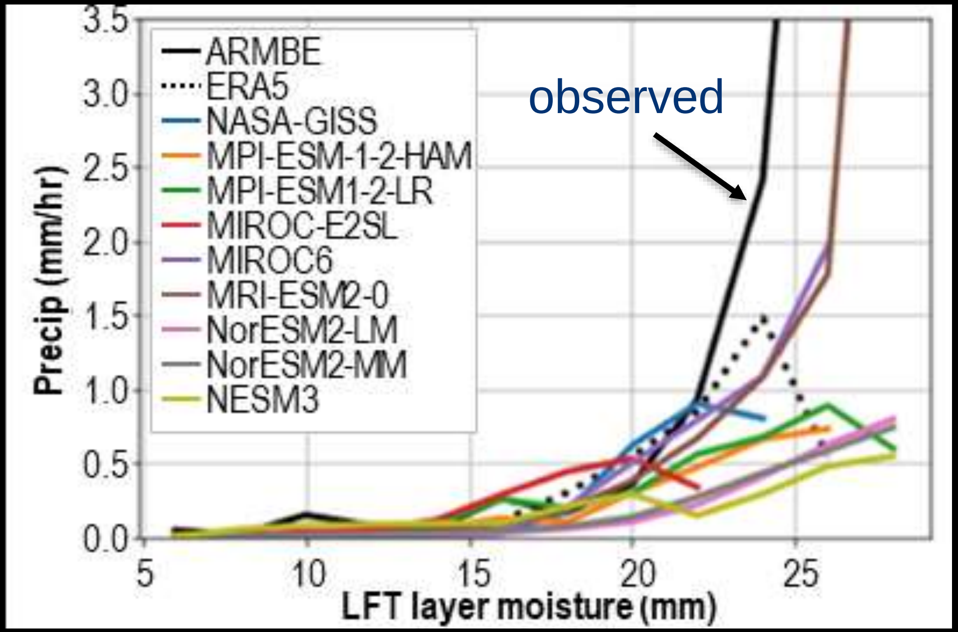

Emmenegger et. al., 2022, in review

Precipitation-water vapor relation guiding model development

Many models "pick up" early (rain too frequently at too low of a rate)

Individual or multiple convective clouds are typically represented as plumes of buoyant air exchanging air through interactions with their environment

Convection initiated if boundary layer air would be warmer than its environment after lifting and mixing:

- Too strong coupling to to surface → convection triggered too easily
- Insufficient sensitivity to moisture through entrainment

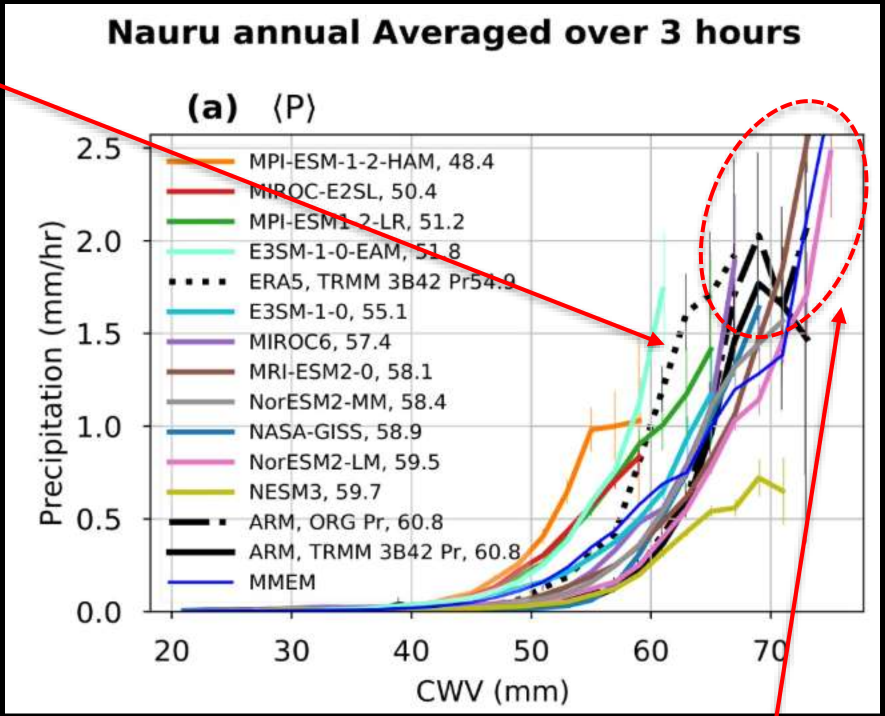

Emmenegger et. al., 2022, in review

Joint global "high precip, high moisture" domain: Conventional satellite observations challenged by attenuation, cloud cover

Global Navigation Satellite System (GNSS) Radio Occultation (RO) Concept

The actual ray path between the transmitter and receiver is slightly longer than the straight line distance

This is largely due to the gradient in the tropospheric temperature and water vapor structure

The separation between the two satellites is accurately known. Precision clocks can derive the "excess phase delay" from consecutive measurements

Senses through heavy precipitation

GNSS Receivers

COSMIC-2
Sentinel-6
GRACE-FO
…….
many commercial

GNSS Systems

GPS (United States)
Glonass (Russia)
Galileo (European)
BeiDou (China)
QZSS (Japan)
NavIC (India)

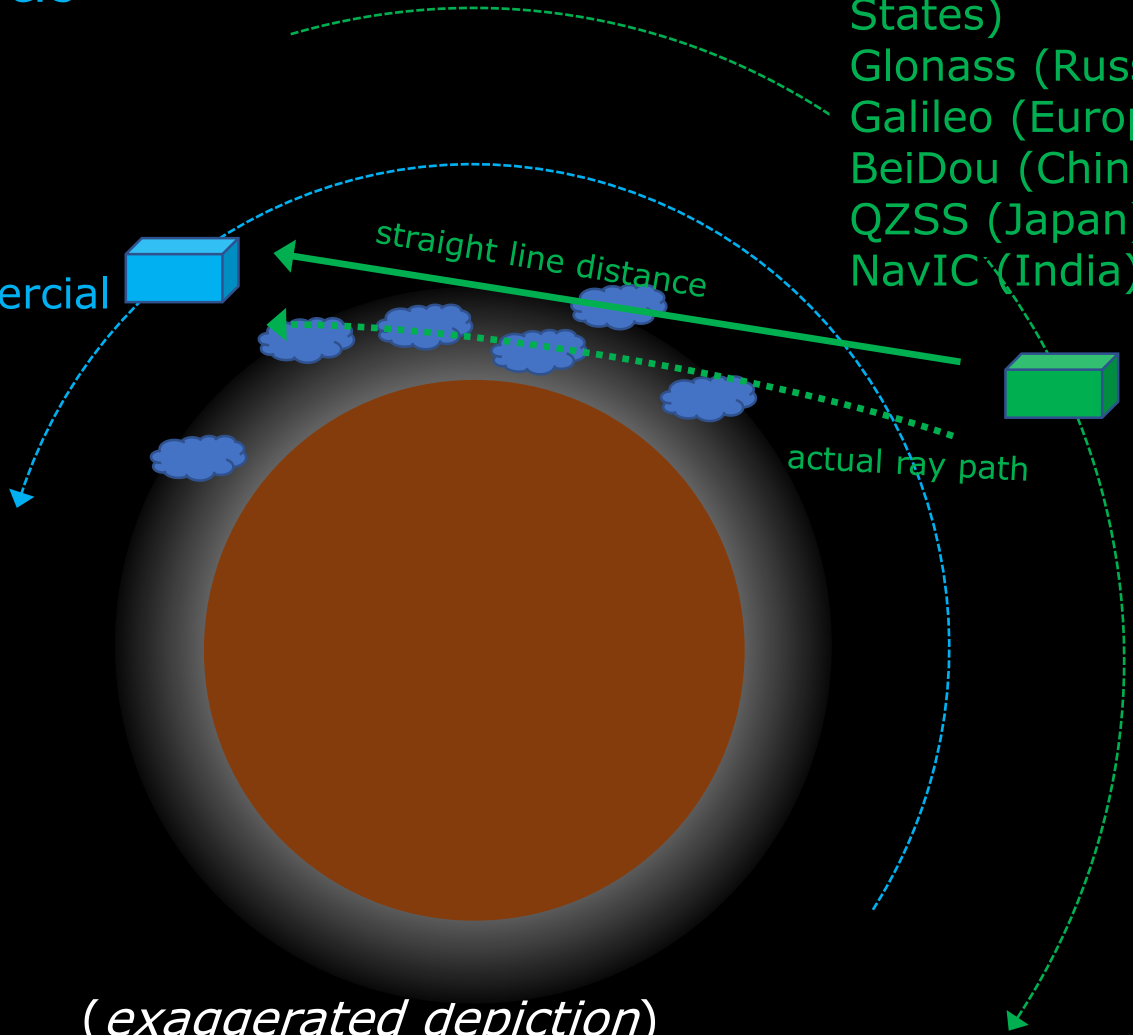

(*exaggerated depiction*)

Global Navigation Satellite System (GNSS) Radio Occultation (RO) Concept

Snell's Law:

$n_1 \sin(\theta_1) = n_2 \sin(\theta_2)$

Bending occurs when the refractive index (n) changes

In the atmosphere, the refractive index changes continuously

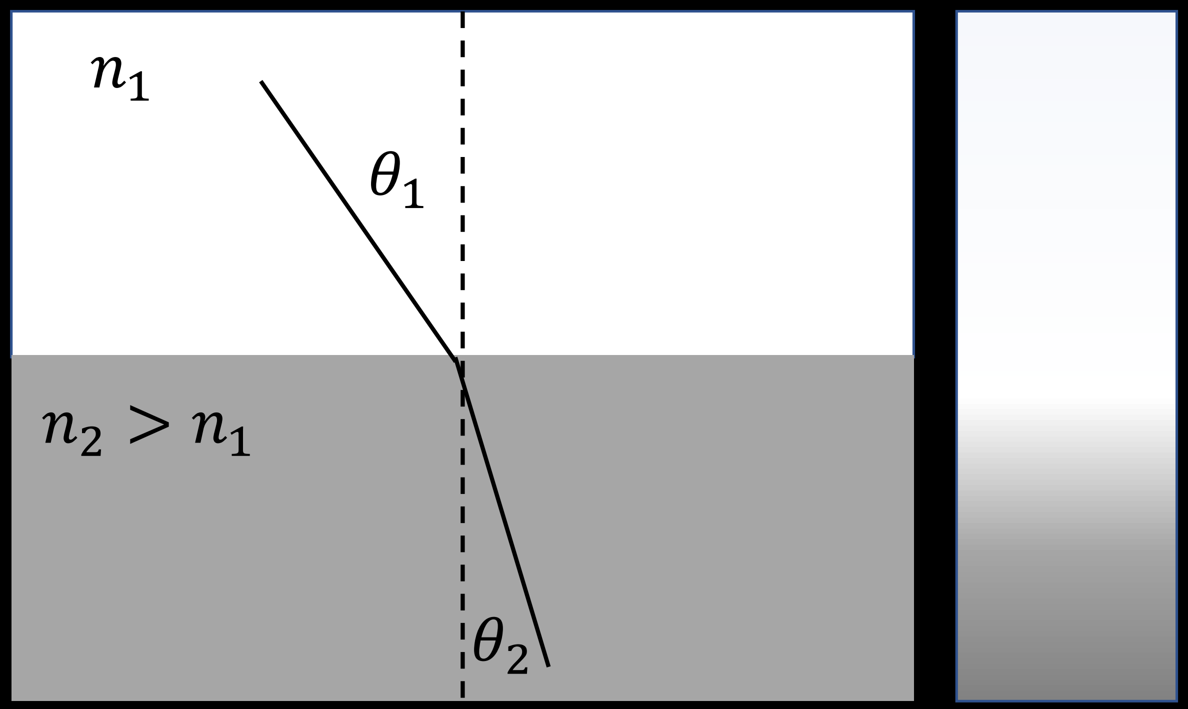

RO Geometry and Terms

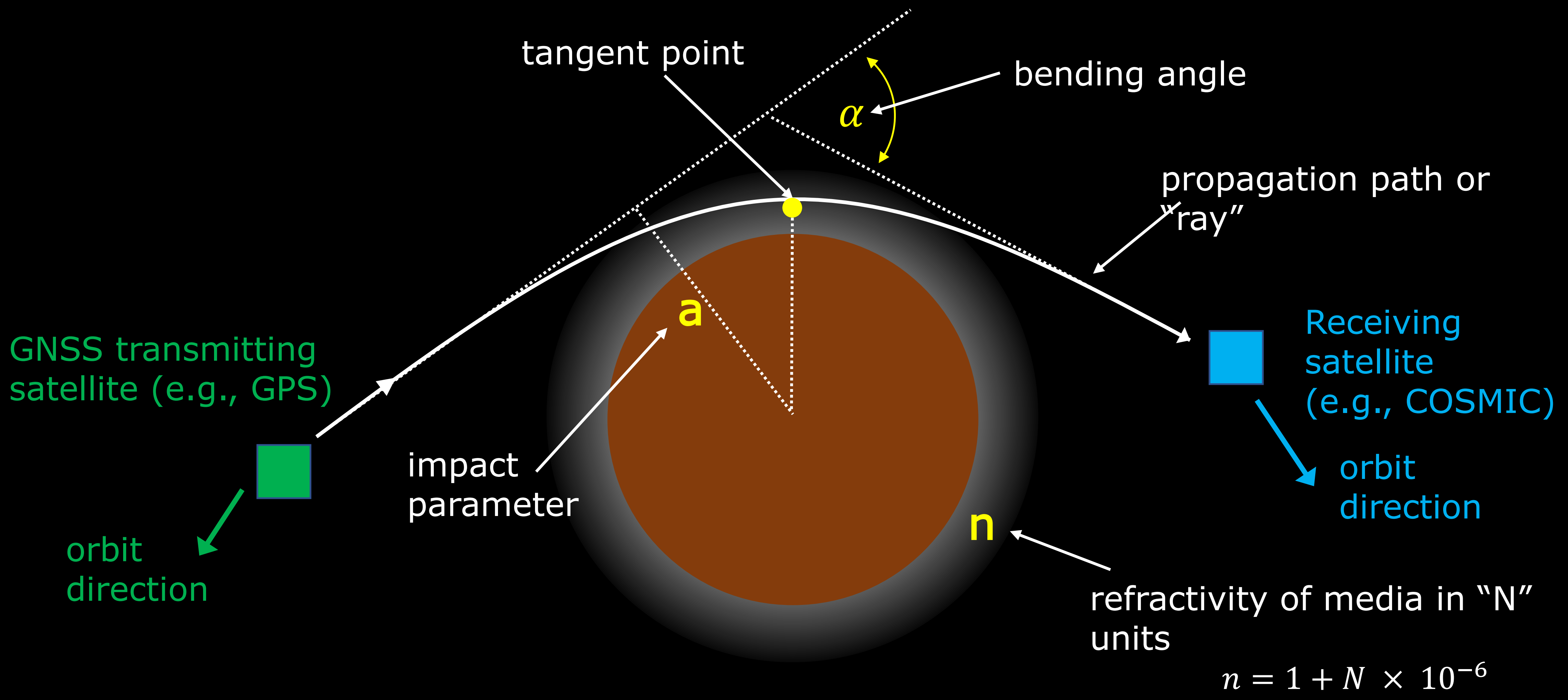

single ray shown (*exaggerated depiction*)

GNSS Radio Occultations (RO) Processing Flow

Dedicated dual L-band (near 1.4 GHz) GNSS receivers track the GNSS phase delay

- The signal is bent due to the index of refraction gradients in the atmosphere
- RO receivers precisely track the time derivative of the phase between consecutive measurements (Doppler shift)
- After removing geometric effects due to relative motion of the two involved satellites, the atmospheric bending angle can be inferred

(*exaggerated depiction*)

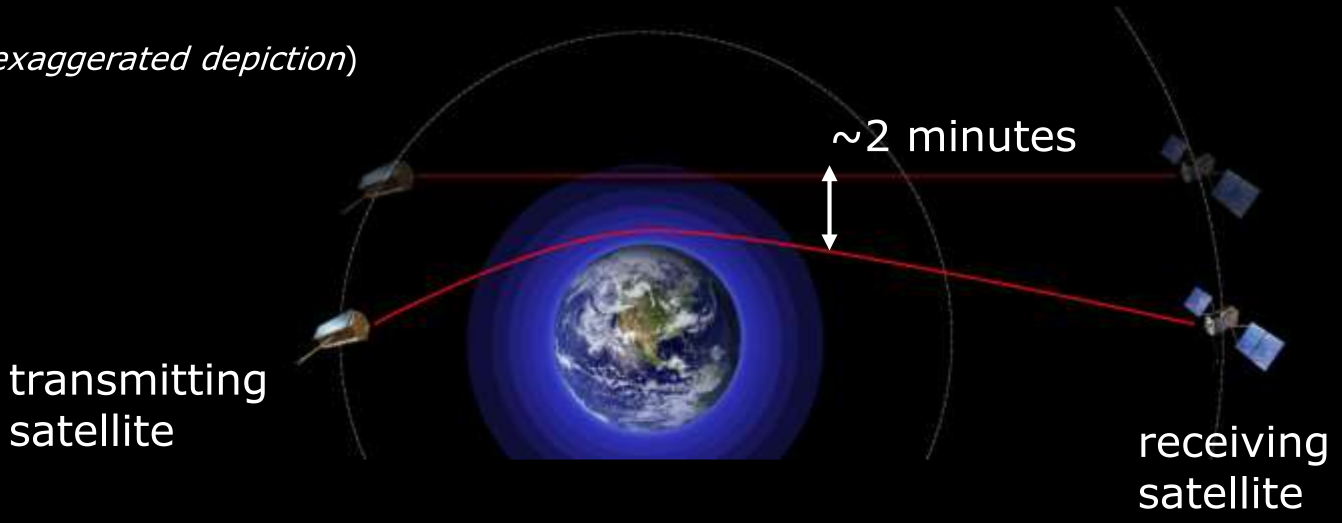

Excess phase

↓

Bending angle α

Spherically symmetric atmosphere ↓ Inverse Abel transform

Index of refraction *n(z)*

Variational analysis ↓ T from models to infer q

T(z), q(z)

- High vertical resolution (~200m), globally distributed
- All-weather capability
- Coarse along-ray resolution

GNSS RO Horizontal Resolution: "Along-ray" Perspective

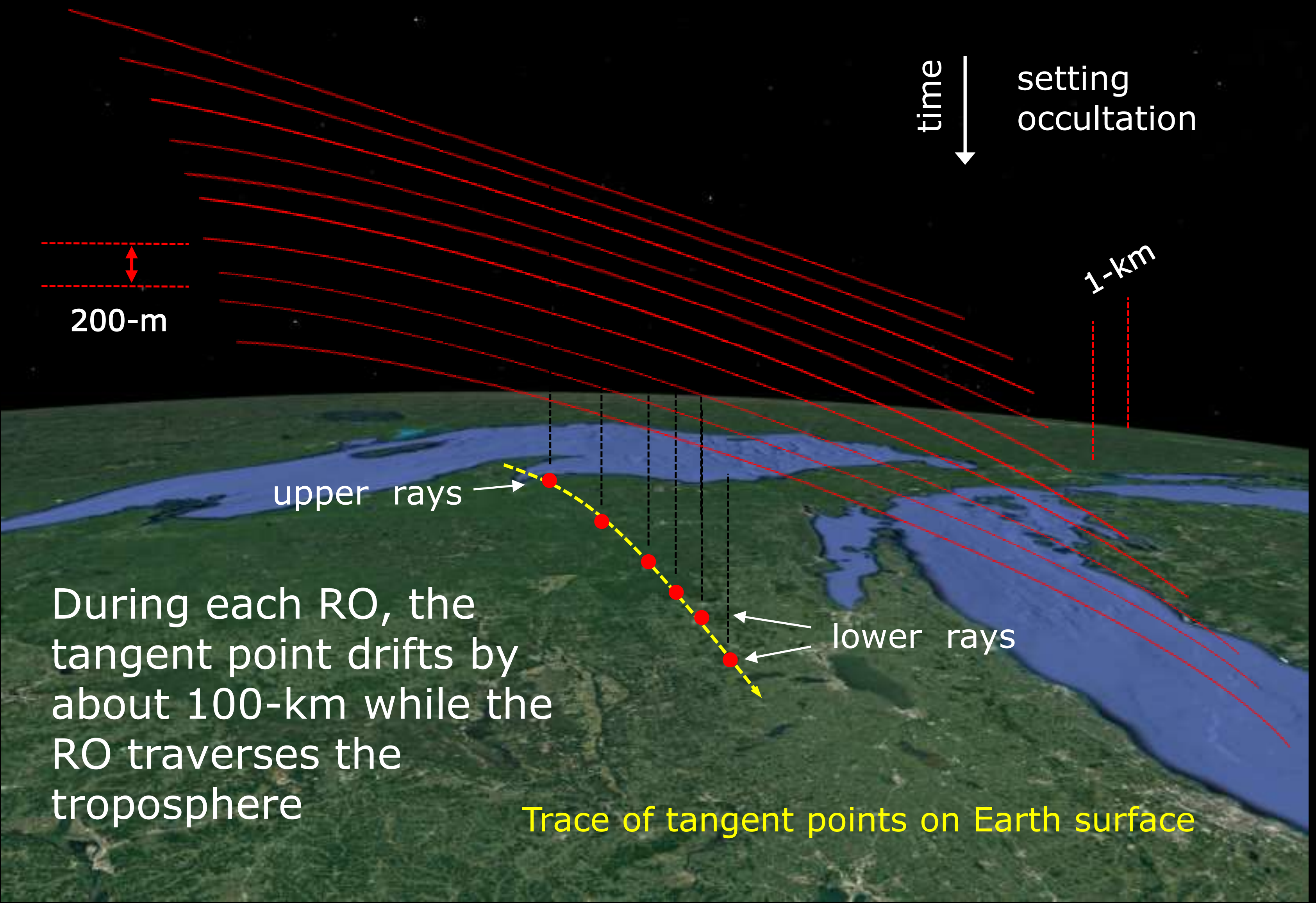

During each RO, the tangent point drifts by about 100-km while the RO traverses the troposphere

Trace of tangent points on Earth surface

The resolution in the vertical is very fine (200 m)

The resolution in the "along-ray" dimension is fairly coarse, 200-km or more

The resolution in the "across-ray" dimension is very fine (1-km), essentially limited by the Fresnel volume along the propagation path

A RO measurement has very high resolution in 2 of the 3 spatial dimensions

(*exaggerated depiction*)

COSMIC-2 Radio Occultation (RO) Sampling Characteristics

The COSMIC-2 satellites are arranged one-per orbit plane, resulting in RO soundings that are spaced far apart on the ground

- COSMIC-2: 6-satellites, 24-deg orbit inclination, 500-km altitude
- These RO observations sense through heavy precipitation, but cannot directly detect the presence/absence of precipitation
- NASA is increasingly obtaining RO data through their Commercial Small Satellite Data Acquisition (CSDA) program
- Once an RO finishes, the Earth rotates before the **same** COSMIC-2 receiving satellite can return for a second RO (viewing the same GNSS transmitting satellite)
- On occasion, a **second (or third)** receiving satellite may occult the same GNSS transmitter, within a time offset relevant to the convective time scale (e.g., 10 mins or less)

Constellation Observing System for Meteorology, Ionosphere and Climate (COSMIC-2)

RO Sampling (Only COSMIC-2) JJA 2022

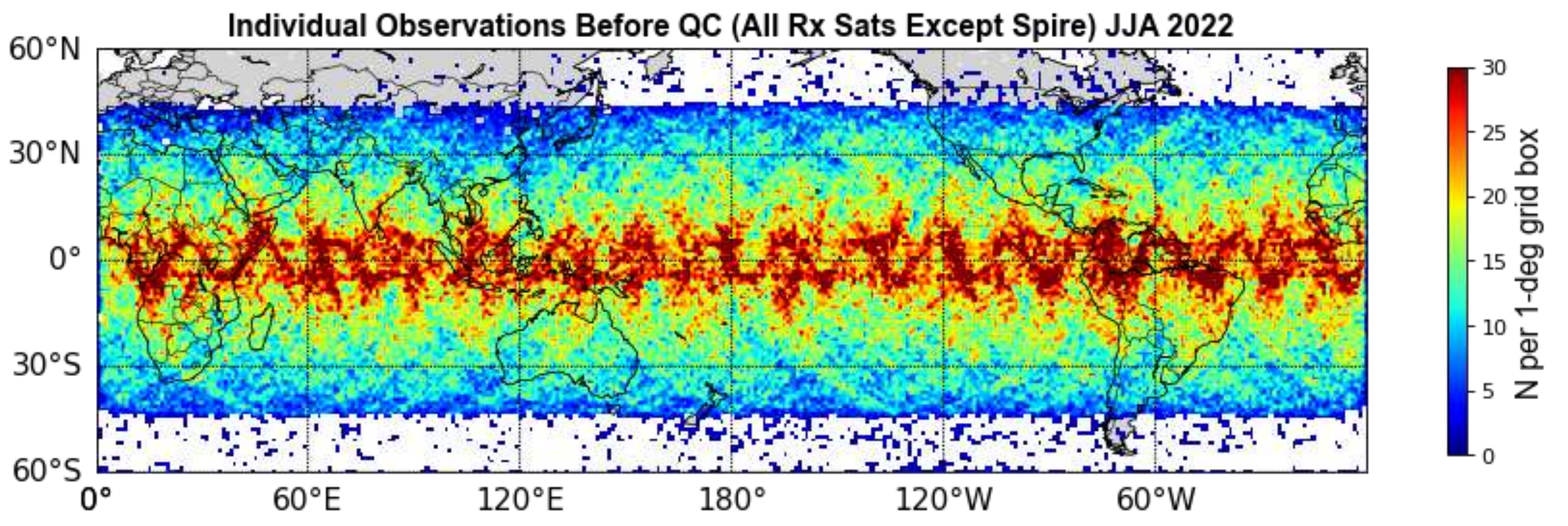

Before QC: All RO, regardless of lowest level

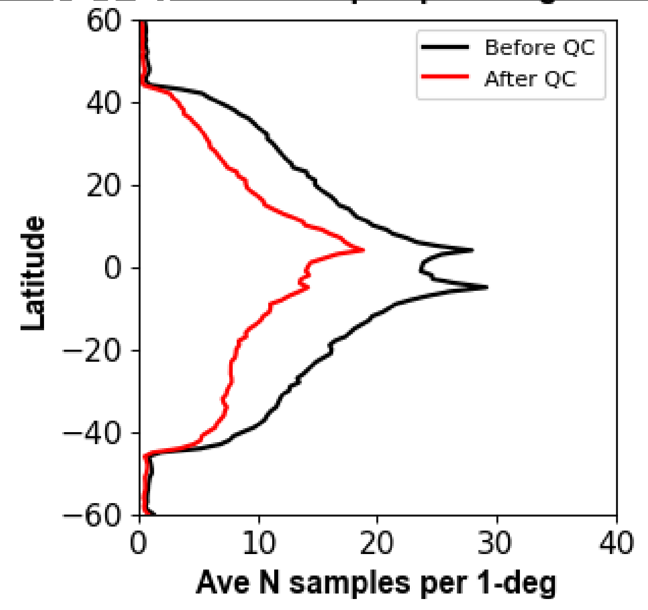

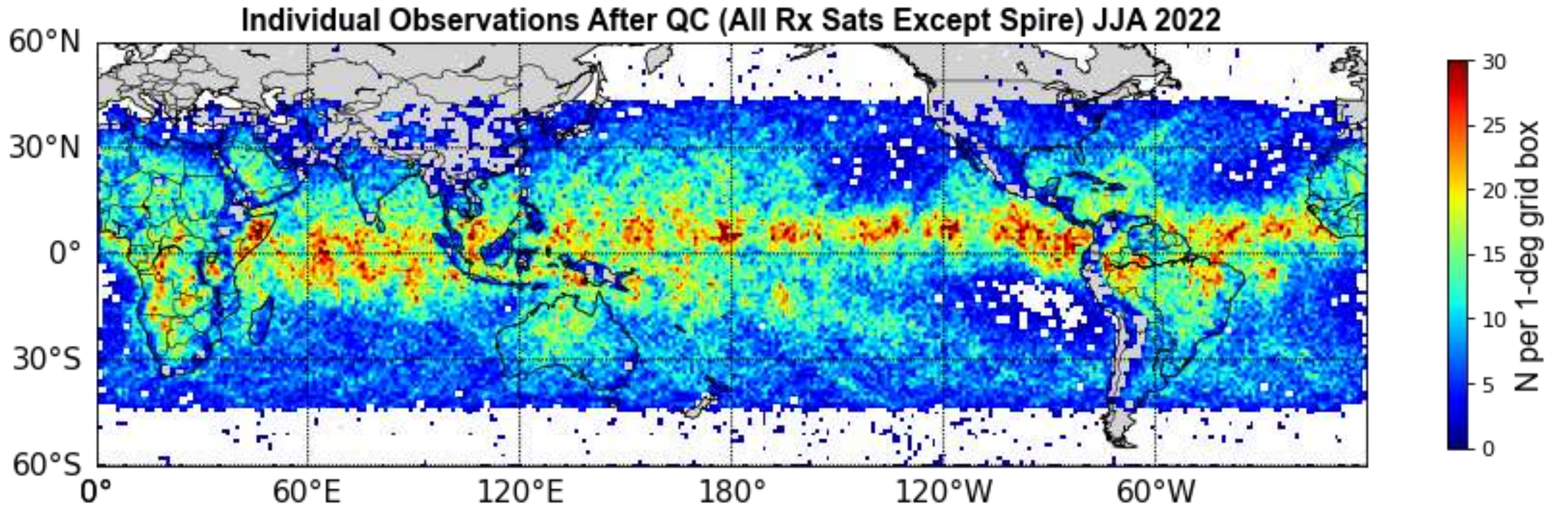

After QC: Only those RO reaching to at least 920 hPa (ocean) or to within 500-m of terrain height (land)

RO Sampling (Including Spire data) JJA 2022

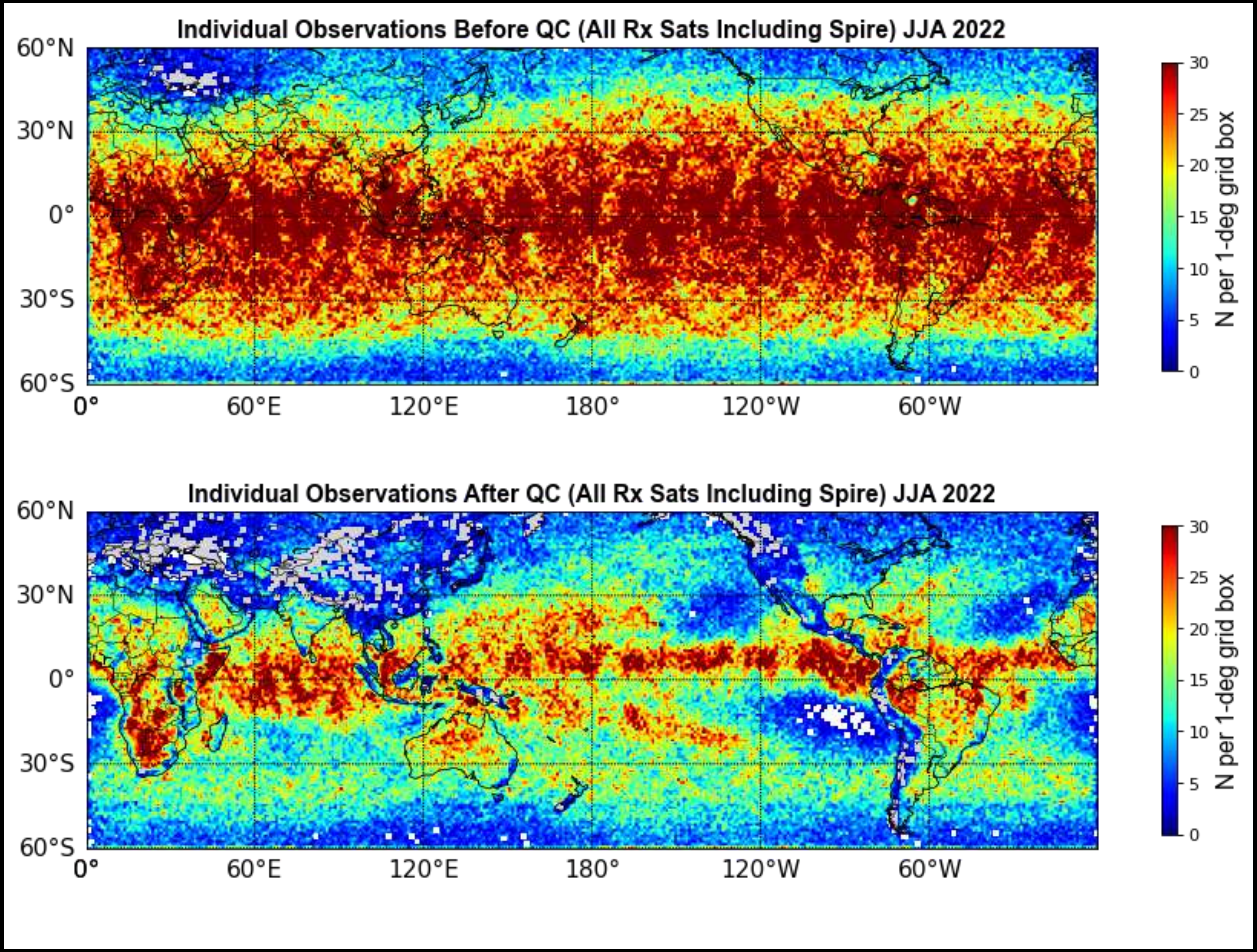

Before QC: All RO, regardless of lowest level

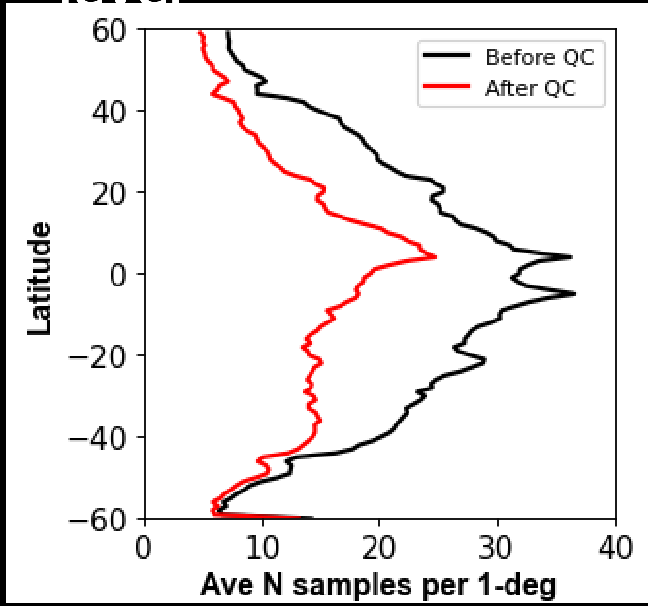

After QC: Only those RO reaching to at least 920 hPa (ocean) or to within 500-m of terrain height (land)

Further Refinement: “Nearby” RO Data (After QC)   JJA 2022

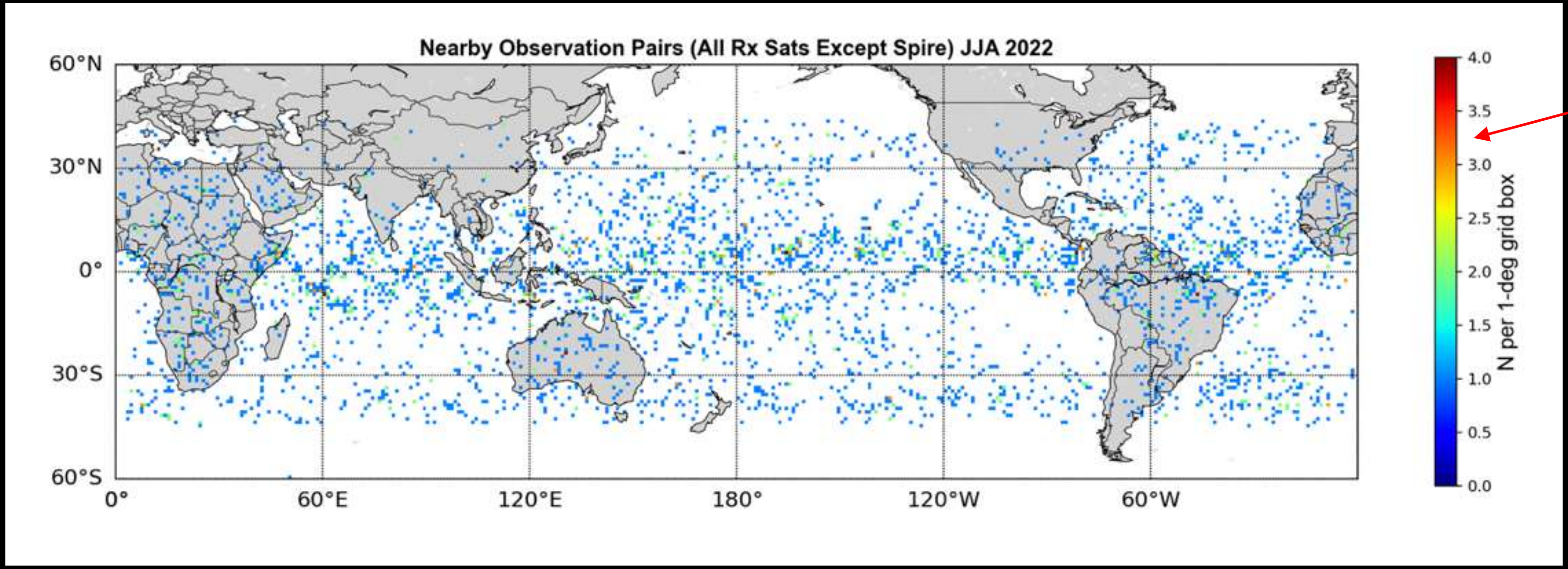

Scale is from 0 to 4

Nearby RO Only COSMIC-2

Whenever two RO occur within ±10 min, 200-km of each other

Without consideration of associated precipitation conditions

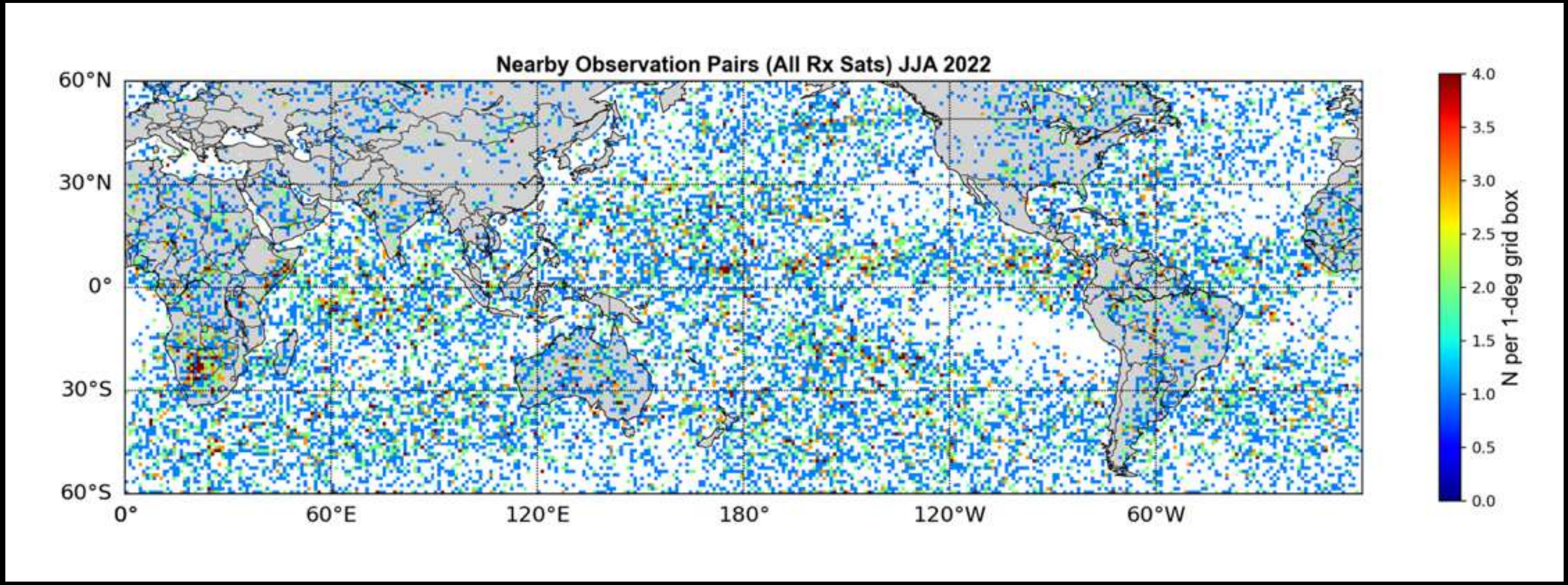

Nearby RO Including Spire

Using vertical profile information to assess convective conditions in CMIP6 models

Few of the models accurately capture the increase of precipitation with environmental moisture

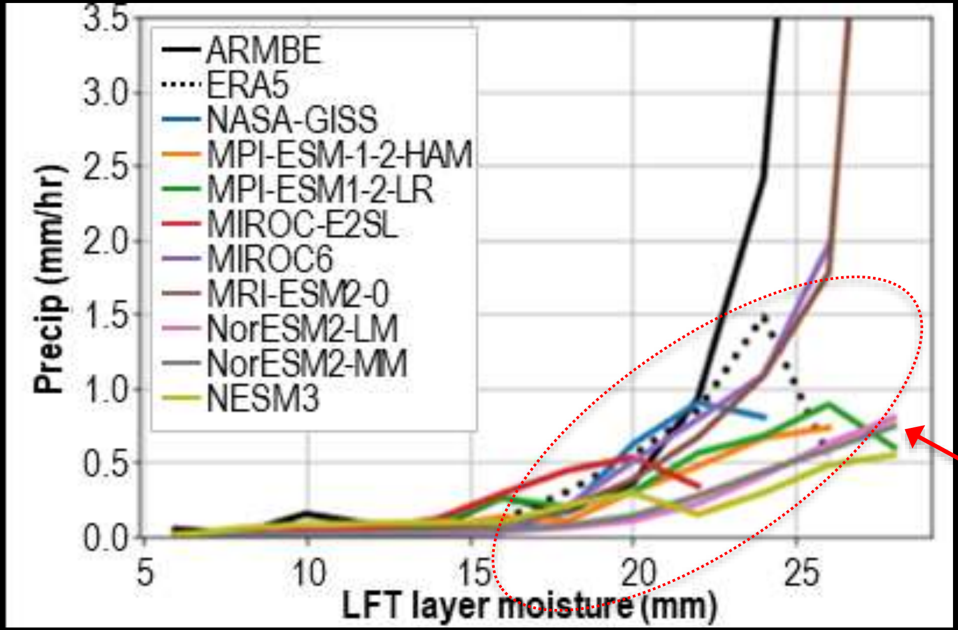

Emmenegger et. al., 2023, in review

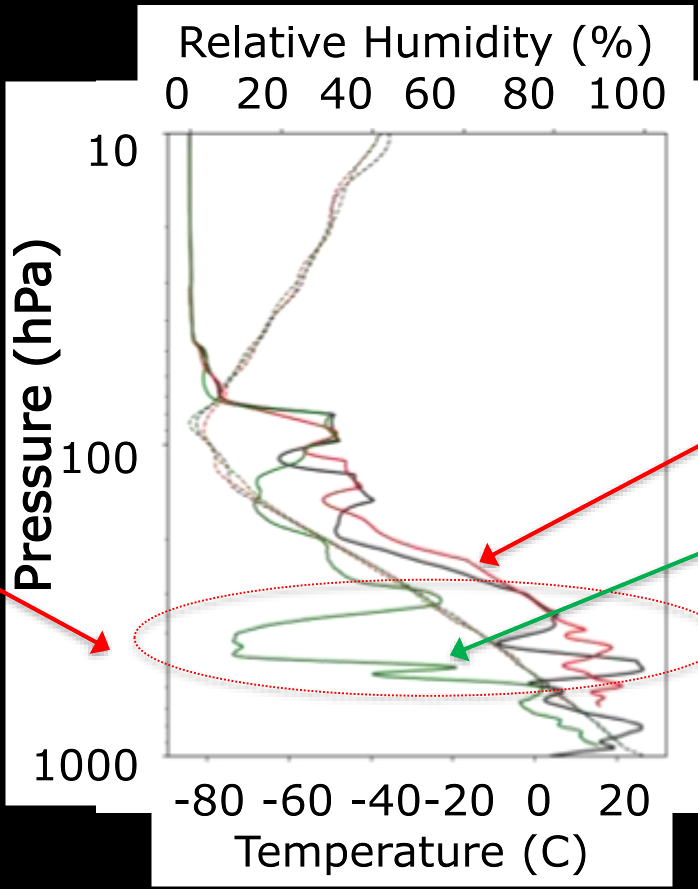

Example from two close-by COSMIC-2 RO

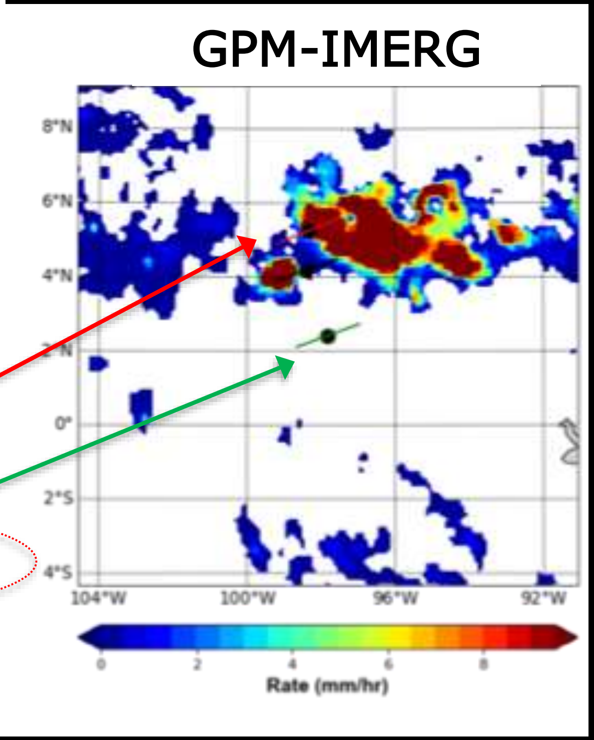

Precipitation conditionally averaged on moisture in the 750-900 hPa layer for in-situ ARM site observations and several CMIP6 models

COSMIC-2 "RO Pairs"
All of 2021
Within ±10-min
< 200-km separation
Over-Ocean
±20-deg latitude

Red= e from RO-1 (inside rain)
Orange= e from RO-2 (outside rain)

Black= e_{sat} from RO-1
Blue= e_{sat} from RO-2

Red/Orange curves diverge, ($e-e_{sat}$) smaller in precip by 5K, relative to ($e-e_{sat}$) outside precip

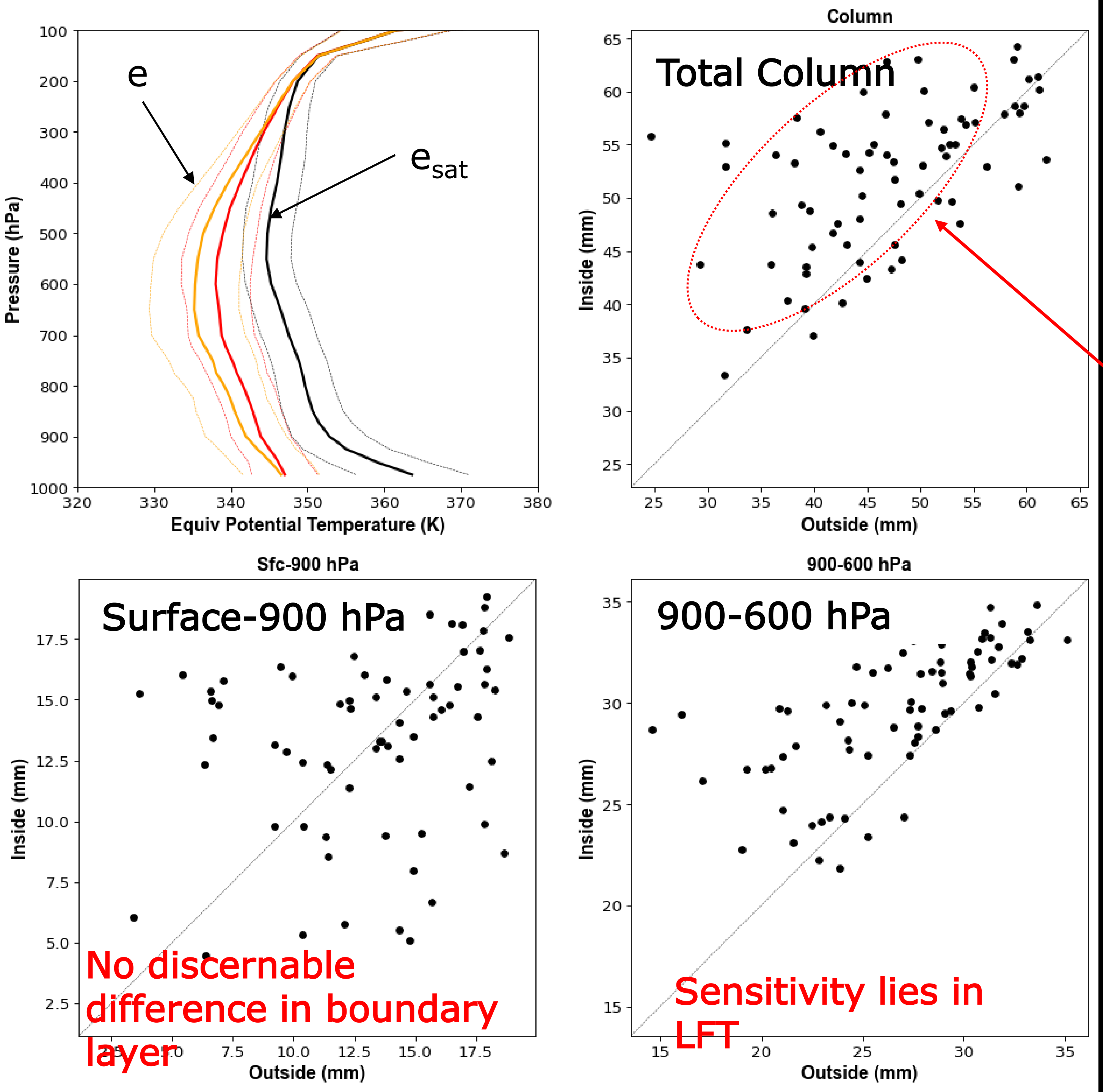

Selection criteria:
RO-1 exceeding 2 mm/hr along-path
RO-2 non-raining

Total column vapor larger for RO "inside" precip - where?

3-month Totals Using UCAR CDAAC Data   JJA 2022

Land and Ocean ±60-deg Latitudes

	Total RO	Total RO After QC	Nearby	Nearby with Rain	Nearby with Rain and No-Rain	Percent ±20 deg latitude
COSMIC-2 (Excluding Spire)	500319	293498	3935	286	21	48
All Data (Including Spire)	895951	551283	23534	1407	141	63

- The number of nearby rain RO profiles is limited, < 1000 events/year
- These are conventional RO, with no capability to directly detect the coincident presence of heavy precipitation

The STORM-PROBE[1] Concept

The STORM-PROBE concept consists of a low-Earth orbiting satellite constellation of GNSS polarimetric RO (PRO) measurements

The receiving satellites are spaced such that adjacent PRO would view the same GNSS transmitting satellite

Captures independent moisture profiles within and in the nearby environment surrounding convection (Turk et al., 2022)

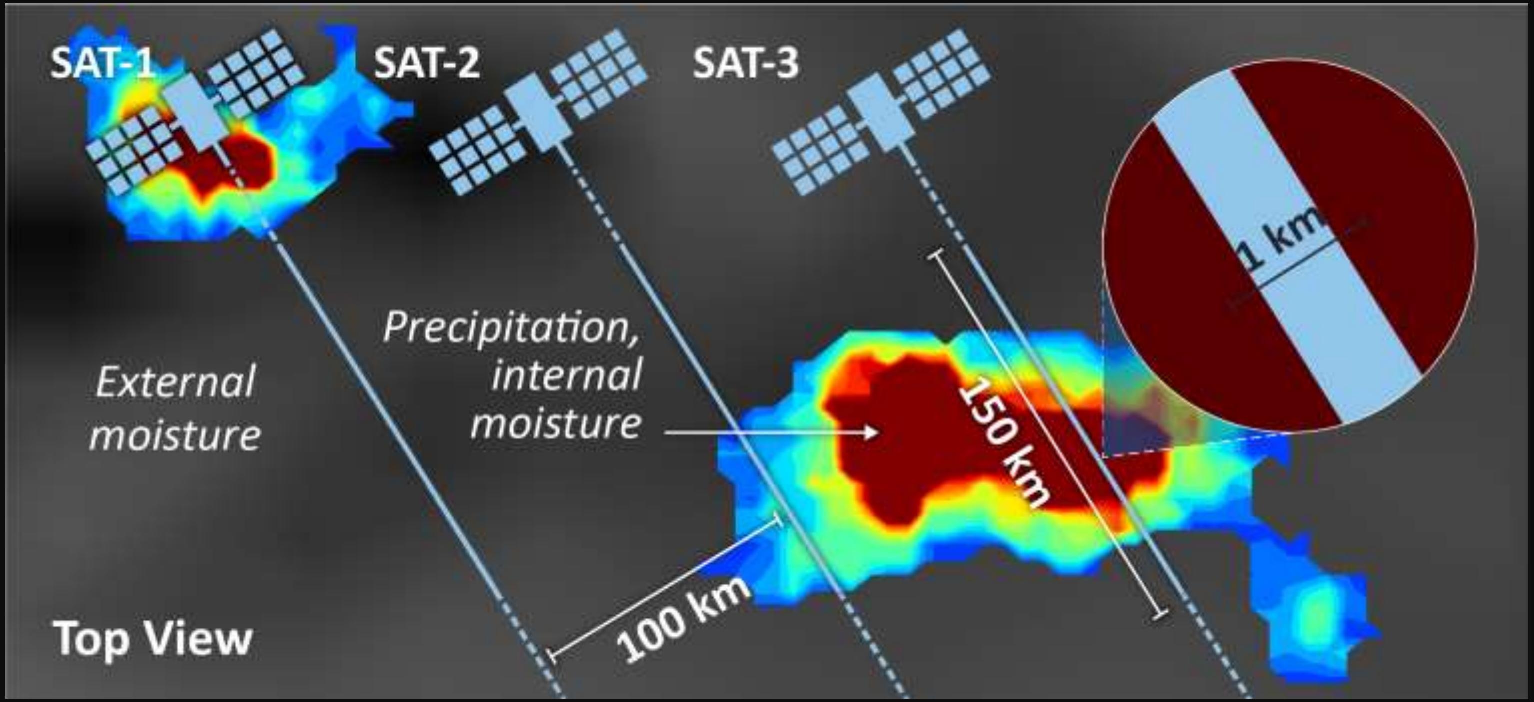

1 Storm Thermodynamic Occultation for the Role of Moisture-Polarimetric Radio OBservations of the Environment

STORM-PROBE Concept

Constellation of three closely-spaced PRO

45-deg inclination
475-km altitude

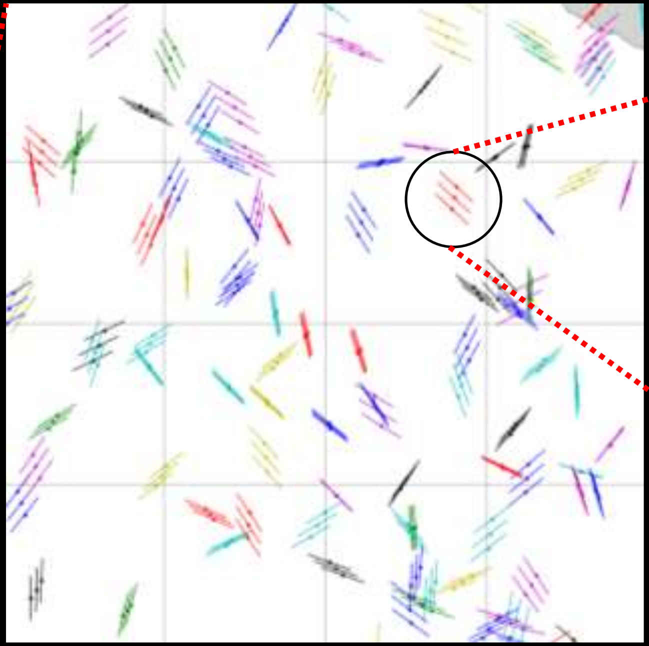

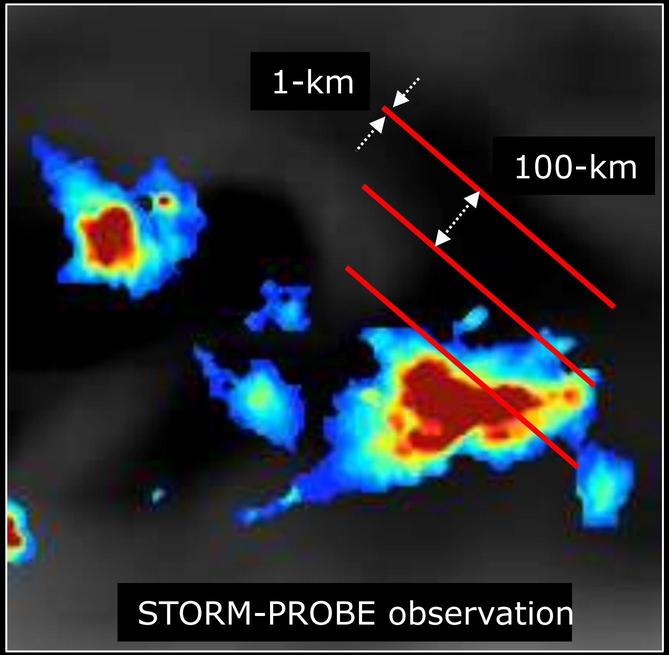

Captures moisture gradient in the "across-ray" direction

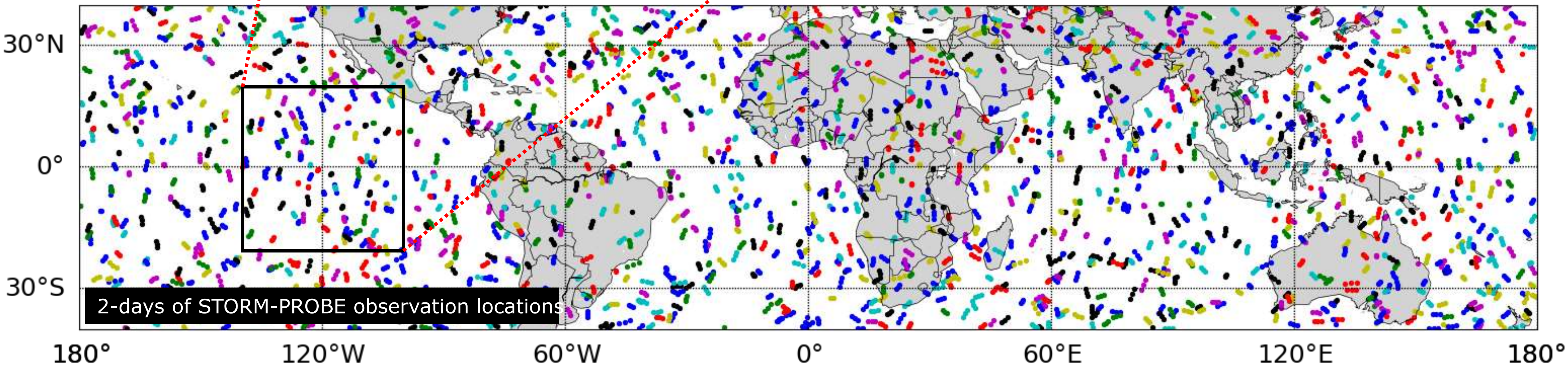

Each STORM-PROBE satellite has an identical dual-polarization GNSS receiver, capturing simultaneous PRO

The STORM-PROBE[1] Concept: Polarimetric RO

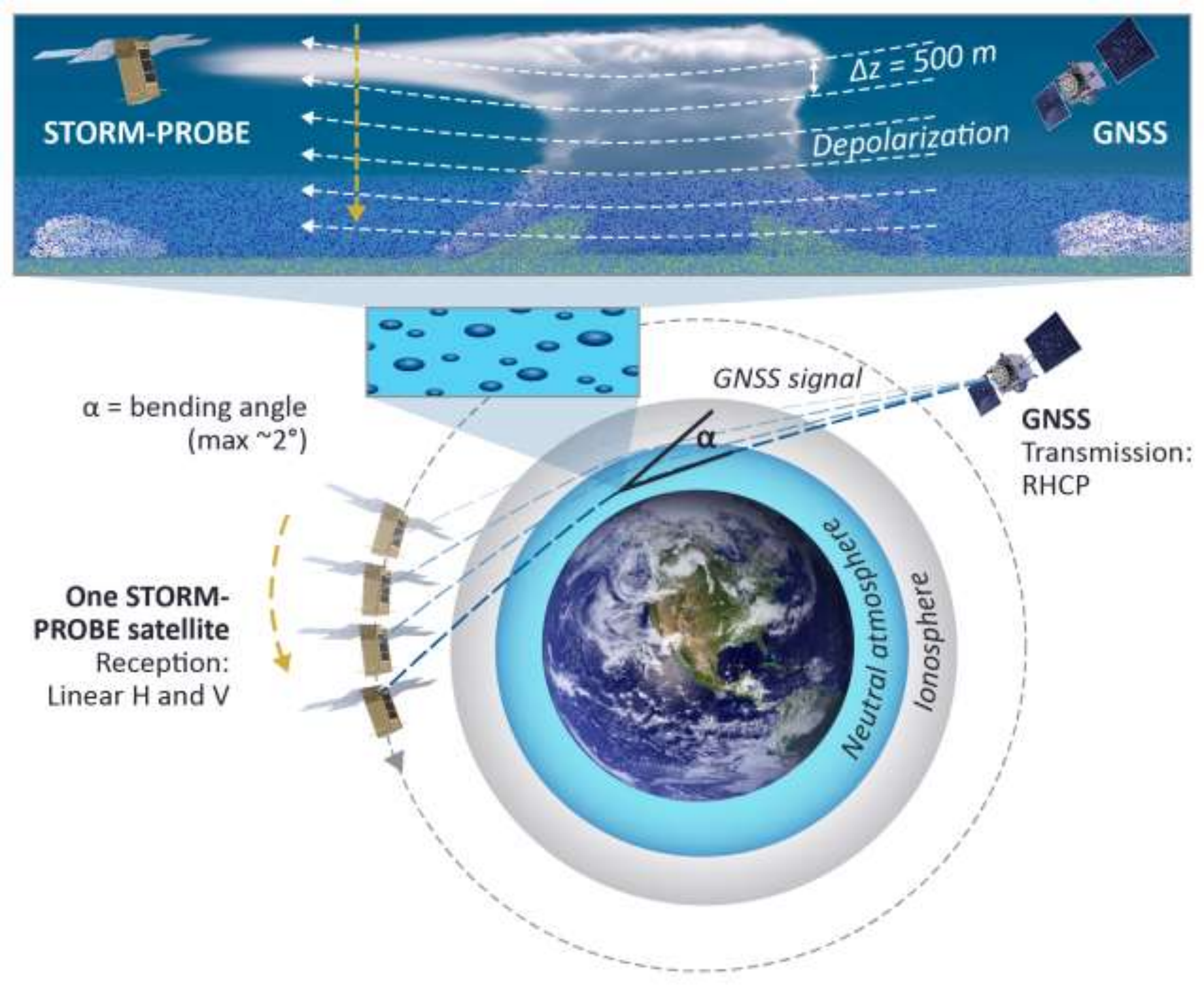

Polarimetric RO (PRO) relies upon hydrometeor shape asymmetry, such that a differential phase time delay ($\Delta\phi$) is induced between the H- and V-polarized GNSS signals propagating through heavy precipitation

The temp/moisture profile and the precipitation detection profile are measured along the identical air mass

PRO concept flight-proven by the Spanish PAZ-ROHP satellite continuously since 2018 (Cardellach et al, 2019)

1 Storm Thermodynamic Occultation for the Role of Moisture-Polarimetric Radio OBservations of the Environment

ROHP-PAZ (Radio Occultation Through Heavy Precipitation with PAZ)

PI: Dr. Estel Cardellach (ICE–CSIC/IEEC, Barcelona)

rohp-PAZ

https://paz.ice.csic.es

JPL participation through the NASA ESUSPI program

- Proof of PRO concept onboard the Spanish PAZ satellite
- Main payload of PAZ is an X-band SAR, operated by Hisdesat for the Spanish government
- Modified IGOR receiver, equipped with dual-pol RO antenna in the aft-direction.
- Launched 22 Feb 2018 from VAFB, CA
- Sun-synchronous 6AM dusk/dawn polar orbit, 514-km
- Polarimetric experiment activated on 10 May 2018
- Averaging 200 RO’s per day, less after early 2020

Dual-polarization antenna

PAZ pre-launch and depiction

Space-X PAZ deployment

Cardellach, E., Tomás, S., Oliveras, S., Padullés, R., Rius, A., De la Torre-Juárez, M., Turk, F.J., Ao, C.O., Kursinski, E.R., Schreiner, B., Ector, D. and Cucurull, L., 2014. Sensitivity of PAZ LEO Polarimetric GNSS Radio-Occultation Experiment to Precipitation Events, *IEEE Trans. Geoscience and Remote Sens.*, 53,190-206, http://doi.org/10.1109/TGRS.2014.2320309

Heritage in Polarimetric Doppler Radar Community

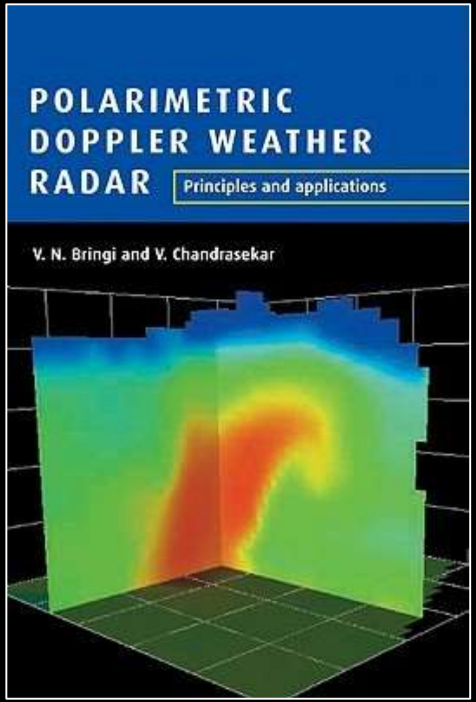

Specific differential phase shift (deg km[-1])

$$k_{DP} = \frac{180}{\lambda} \int Re(f_H - f_V)\, N(D)dD$$

forward scattering amplitudes

Propagation differential phase shift (deg)

$$\phi_{DP} = 2 \int_{r_1}^{r_2} k_{DP}(r)dr$$

Analogous to the polarimetric RO Δϕ measureable

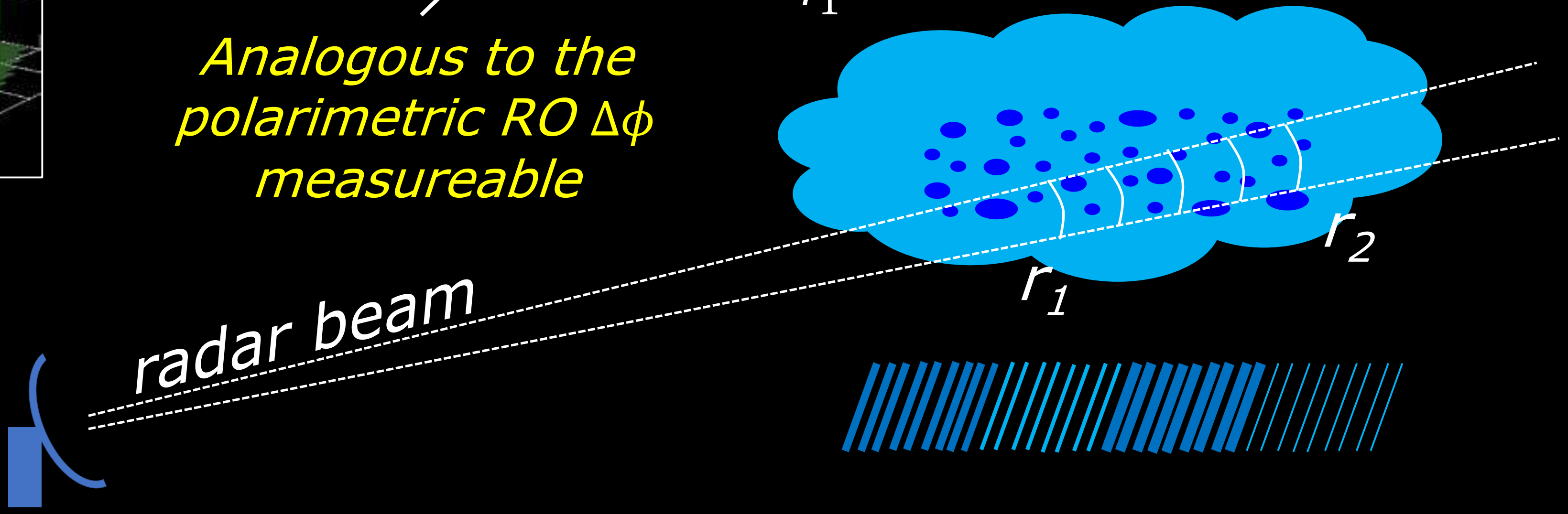

N(D)= hydrometeor size distribution within each radar pulse volume

NEXRAD ground-based radars

(exaggerated depiction)

Relating Polarimetric Phase Difference to Precipitation

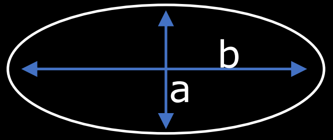

axis ratio= a/b

At 1.4 GHz, K_{dp}-M relationships are nearly linear (solid lines)

$\Delta\phi$ = 10-mm results from 100-km propagation through rain with M= 0.5 g m^{-3} (about 20 mm/hr)

Or from 40-km propagation distance through rain with M= 1 g m^{-3} (about 50 mm/hr)…….

Different combinations of path length and rain intensities yield similar $\Delta\phi$

ROHP sensitivity threshold is about 2-mm, but large signals (> 10-mm) noticed when propagation through mixed-phase and ice

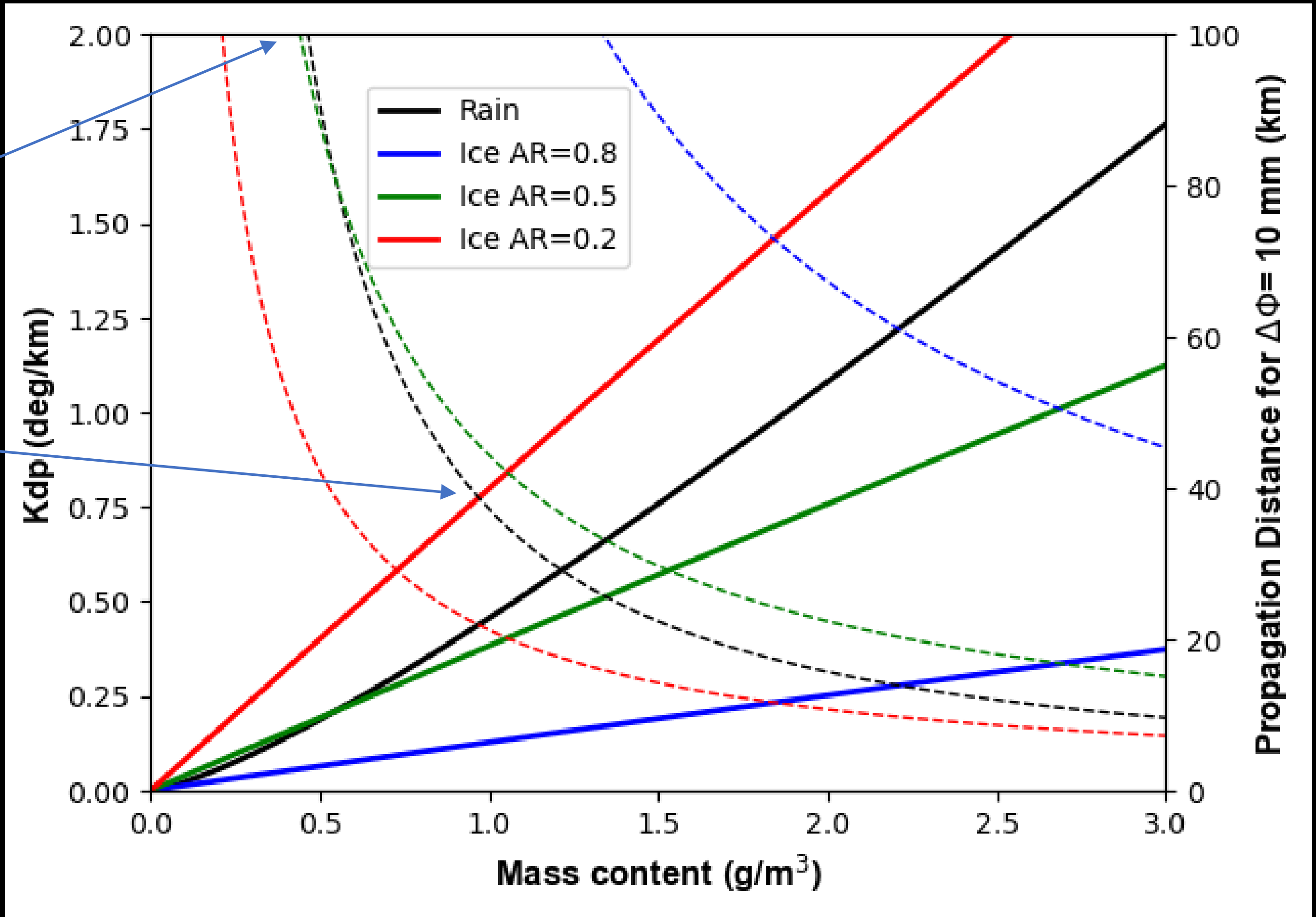

Turk et al., 2021, J. Atmos. Ocean. Tech. https://doi.org/10.1175/JTECH-D-21-0044.1

ROHP-GPM coincidence event 16 March 2019 0934 UTC

Southern Brazil - area where the strongest thunderstorms are known to exist

Observed ROHP $\Delta\phi$ extends much higher than any simulation can re

Height (km)

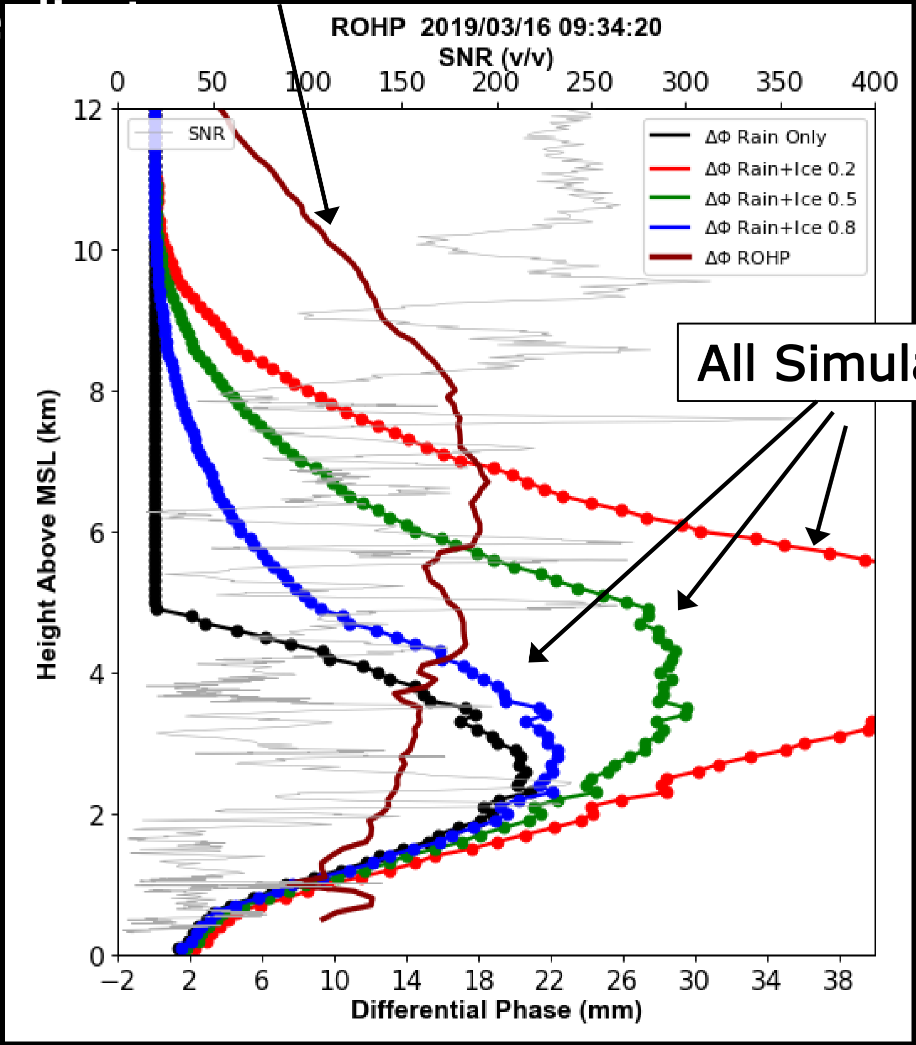

All Simulated $\Delta\phi$

Very cold GMI TB < 150

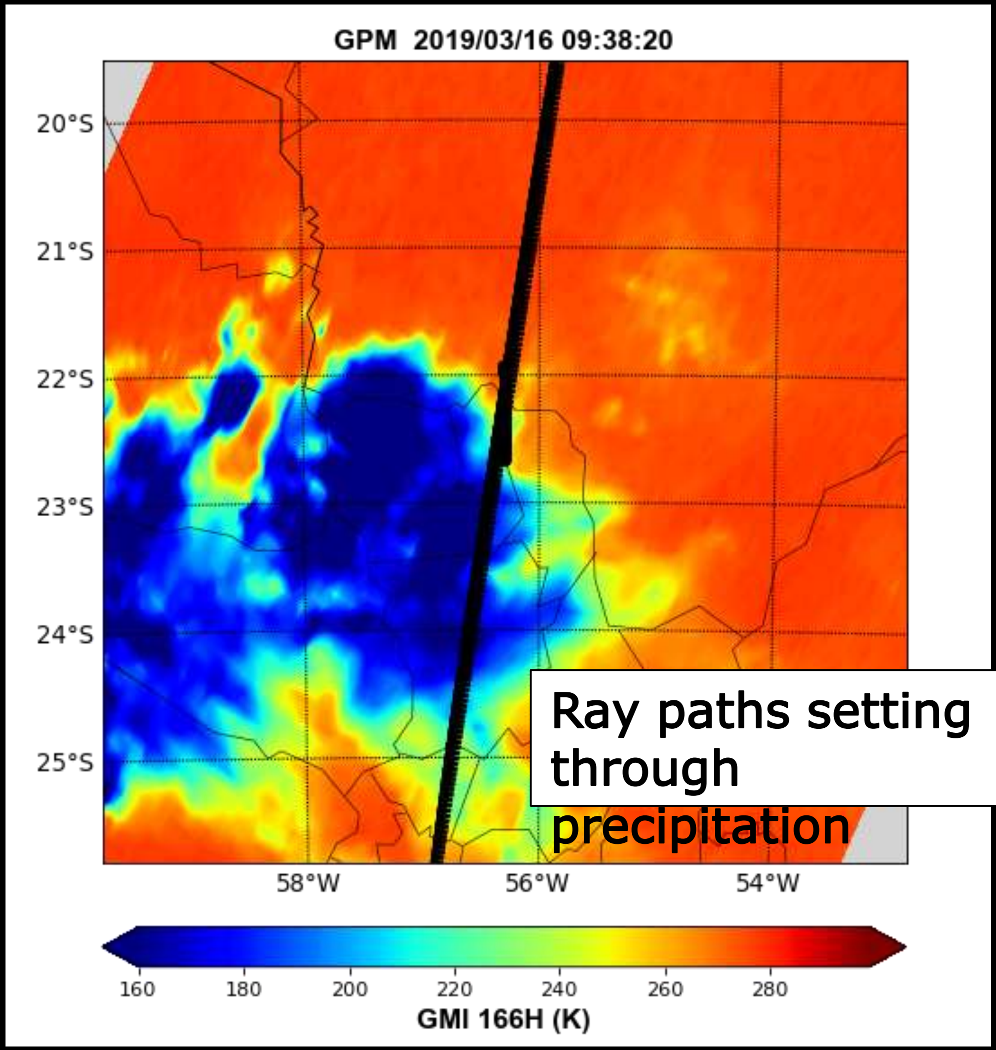

Ray paths setting through precipitation

Precipitation Climatology

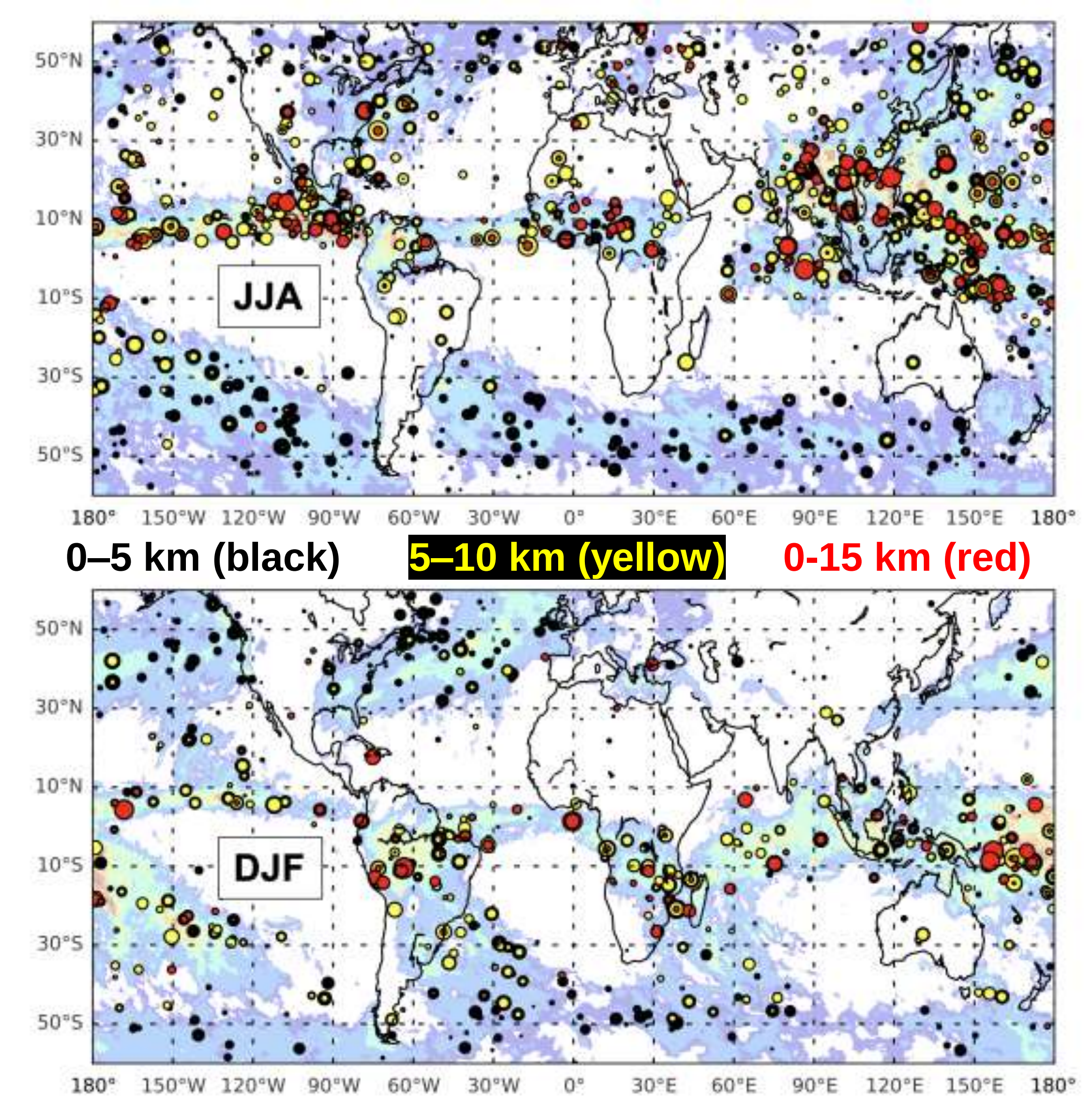

Geographical distribution of the upper percentile (top 2%) of the measured polarimetric phase shift ($\Delta\varphi$) from all ROHP observations

Each dot color denotes a vertical region where the $\Delta\varphi$ from all rays were averaged

The color contour background is GPM-IMERG averaged over the same 3-month period

Geographical agreement with known global precipitation patterns

$\Delta\varphi$ adds an indication of vertical precipitation structure to the (*T, q, p*) profile

Applications: Tropical Meteorology

Potential relevance to NOAA HRD APHEX (Zawislak et al 2022) initiative, for the pre-TD and "invest" regions (observations of low/mid-tropospheric humidity in the near-disturbance environment)

Locations of desired airborne dropsonde observations may be out of reach, or involve considerable ferry, limiting on-station time; pilots avoid convection → dropsondes sample the perimeter

Fortuitous STORM-PROBE observations could potentially complement dropsonde observations

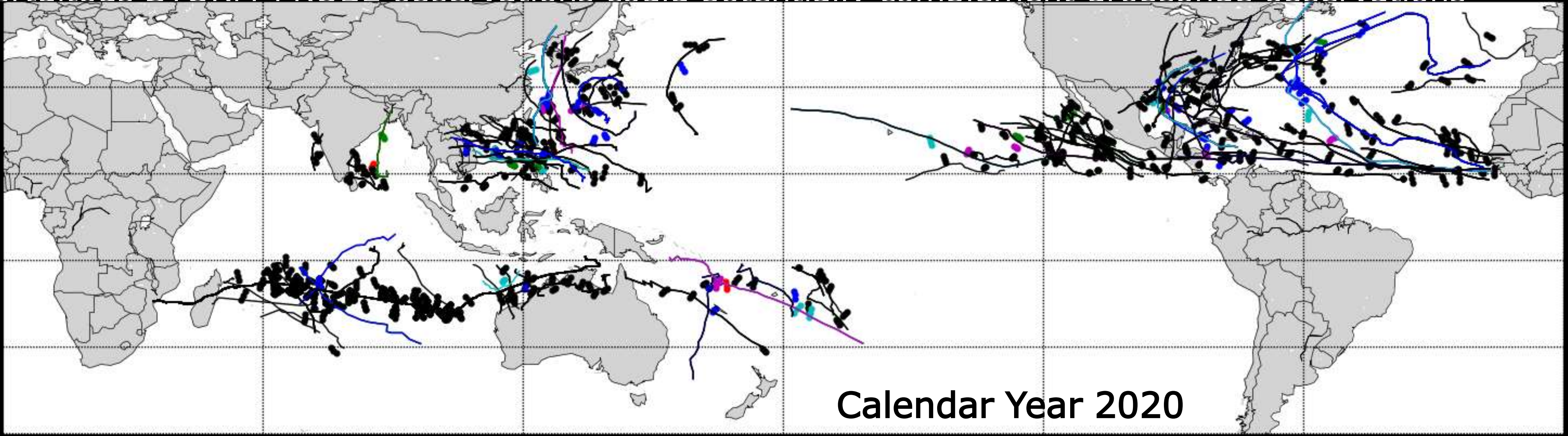

Applications to Tropical Meteorology: Developing TC's

Entire Calendar Year

	All Ocean Basins						Only Atlantic					
Year	**Dep**	**Cat-1**	**Cat-2**	**Cat-3**	**Cat-4**	**Cat-5**	**Dep**	**Cat-1**	**Cat-2**	**Cat-3**	**Cat-4**	**Cat-5**
2019	253	25	15	23	10	3	57	4	5	5	0	0
2020	433	33	8	10	11	3	97	15	2	3	4	0
2021	234	25	5	13	13	1	65	7	0	4	2	0

June-November Only

	All Ocean Basins						Only Atlantic					
Year	**Dep**	**Cat-1**	**Cat-2**	**Cat-3**	**Cat-4**	**Cat-5**	**Dep**	**Cat-1**	**Cat-2**	**Cat-3**	**Cat-4**	**Cat-5**
2019	182	10	4	16	5	0	49	3	2	4	0	0
2020	250	20	2	7	5	1	88	9	0	0	3	0
2021	200	14	8	7	5	1	54	6	1	4	3	

STORM-PROBE simulation, GPS+GLONASS, 3-sats, 45-deg, 475-km
N of observations within proximity of TC location (at least one RO within 200-km of best track)

Applications: Moisture and "Depth" of Convection

Use the top-most level where $\Delta\phi$ exceeds a threshold value above the freezing level (proxy for "radar cloud top")

Would pinpoint layer-sensitivity to the LFT water vapor structure, as strength or "depth" of convection increases

All ROHP, Separated by Height of Top-Most Temperature Level where $\Delta\phi$ > 3-

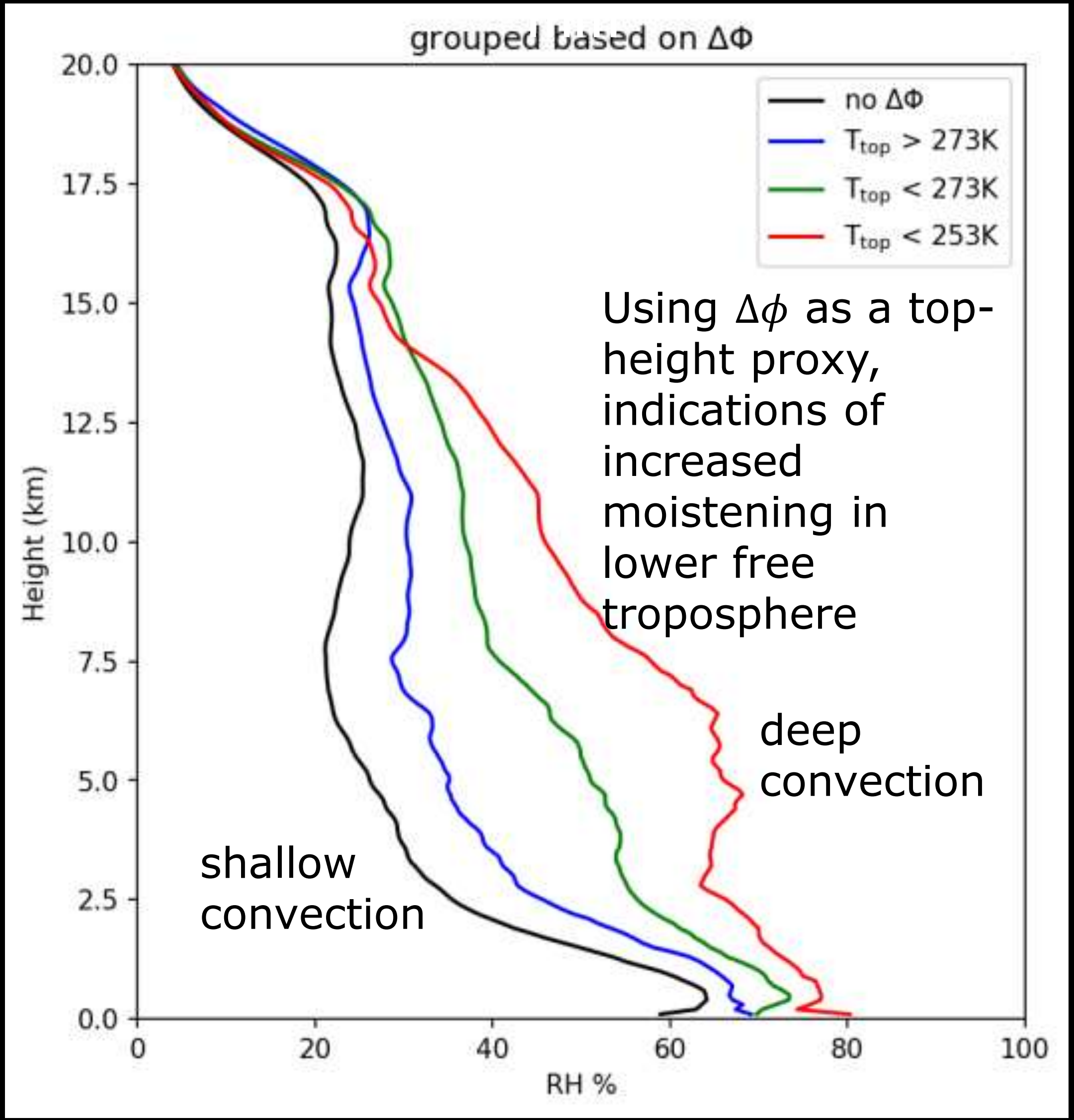

Ice Crystal Scattering- Shape Assumptions

Simulations require specifying the drop size distribution (DSD)

Axis ratio vs equivalent diameter relation for rain is sufficient, but ice can take on complex shapes and varying density

At L-band nearly all hydrometeors are Rayleigh-sized

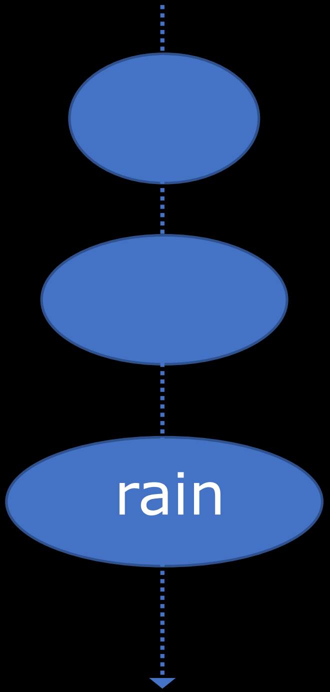

GNSS 1.4 GHz (λ = 19-cm)

GMI 165 GHz channel (λ = 1.8-mm)

aggregate

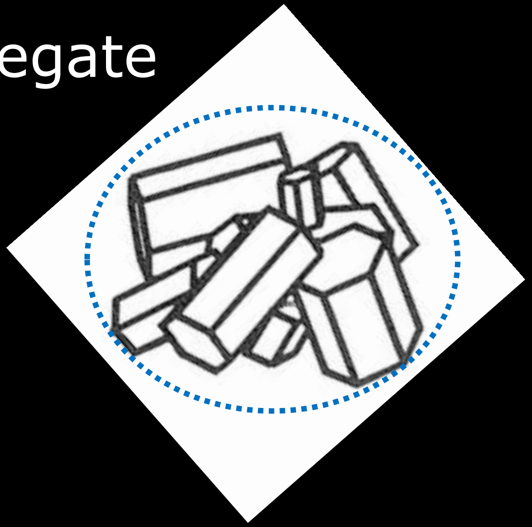

inscribed ellipse

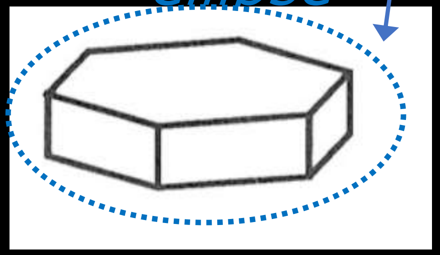

plate

simplifications of actual ice and snow crystals

bullet

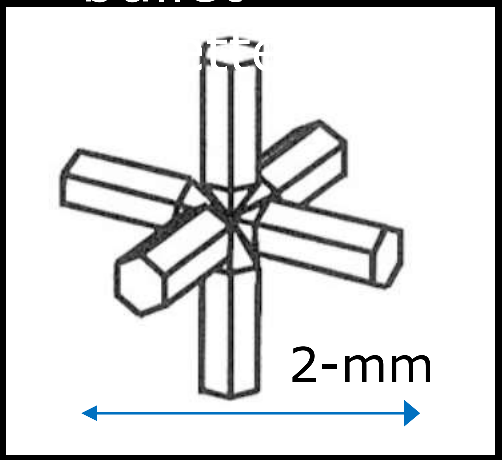

colum

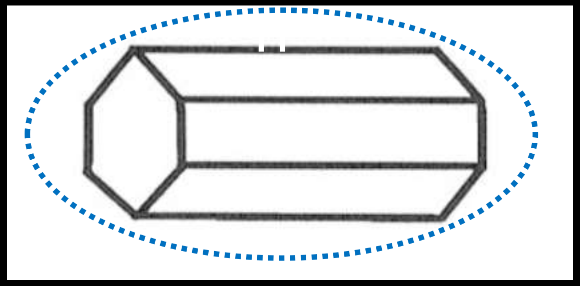

Ice Crystal Scattering- Shape Assumptions

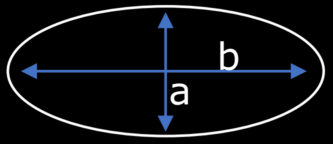

High-density (approaching pure ice) and low axis ratio spheroids agree better with single pristine ice crystals

Low-density spheroids (with a relatively wide range of axis ratio) agree with the results using aggregates

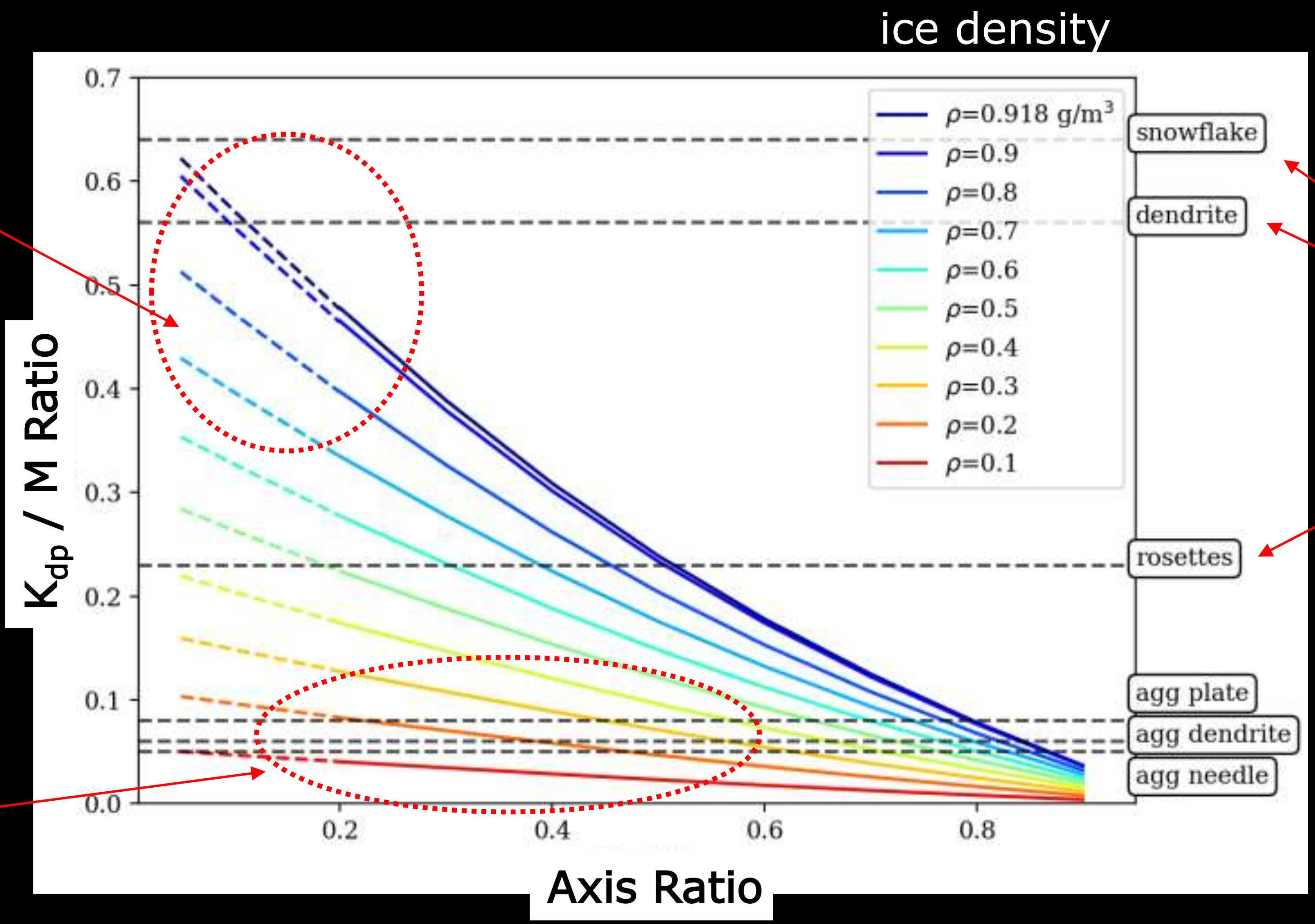

Computed with ADDA (*Yurkin and Hoekstra*, 2011)

(Figure courtesy Ramon Padulles)

The long wavelength (19-cm) favors the agreement found using simple k_{dp}-M approximations (power-law relationships sufficient)

Applications: Integrated Ice Water Path

Δϕ is measured from a coarse (~200-km path) horizontal scale limb-sounding perspective:

- The observation is "naturally averaged" for the user, who may re-grid other finer scale data anyhow to match model horizontal scales
- Upper levels avoids propagation through mixed-phase or rain below; direct sensing of upper level ice

Δϕ and M dependent upon 3rd moment of the DSD

Δϕ shown to be capable of (precipitation-sized) ice water path estimates; recent paper by Ramon Padulles et al (using CloudSat data): https://doi.org/10.5194/acp-2022-300

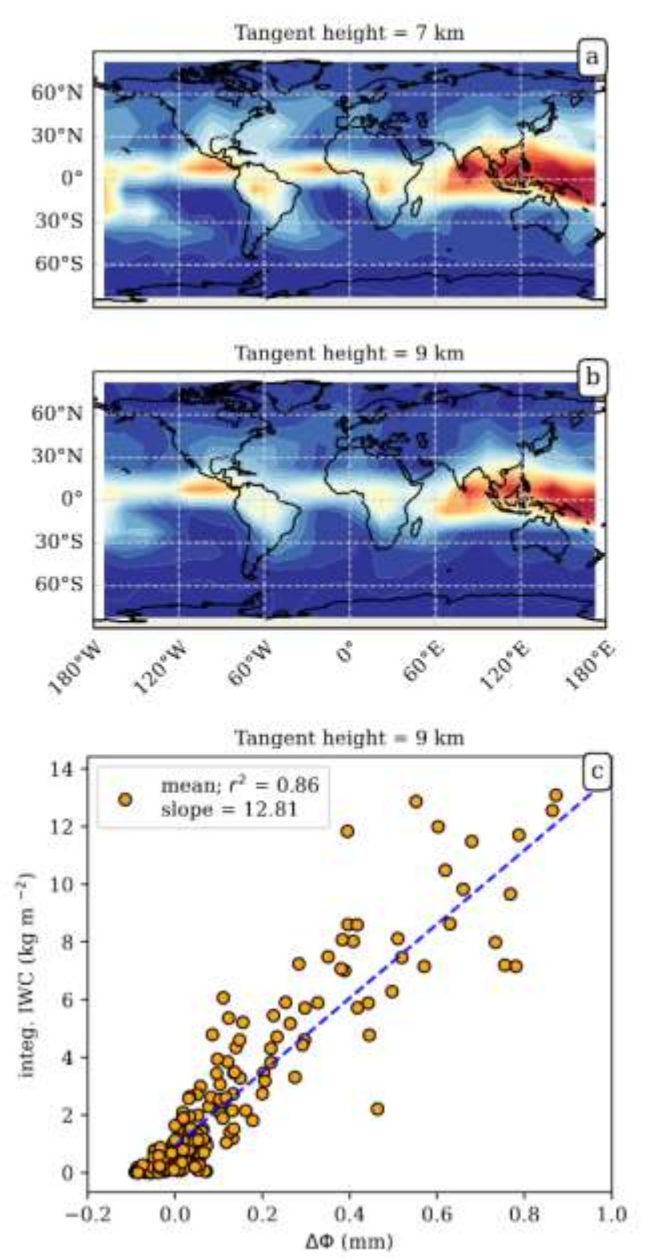

Applications: Weather Model Diagnostics

Evaluation of model bias under heavy precipitation conditions is often done by conditioning upon independent precipitation data (e.g., GPM IMERG, TRMM, etc)

Δϕ signal is coincident with the moisture observation, independent, not (currently) assimilated

Pinpoint details of model bias under heavy precipitation conditions.

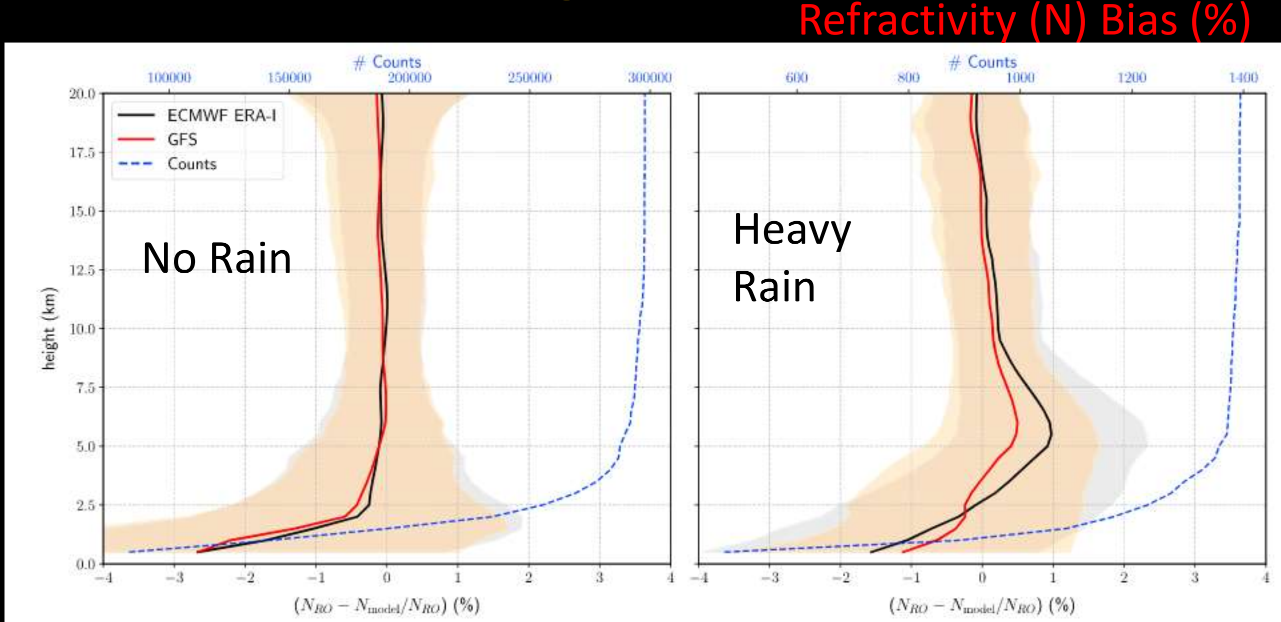

Figure 1. Comparison between Constellation Observing System for Meteorology, Ionosphere and Climate refractivity profiles and weather models in the presence of precipitation versus absence of precipitation according to the Integrated Multi-Satellite Retrievals for the Global Precipitation Mission data product. Left shows the mean (line) and standard deviation (shaded area) differences between the measured and the analysis and reanalysis *N* without rain. Right shows the same analysis for cases with heavy rain. The RO profiles compare to an analysis and a reanalysis (red, GFS, and black, ECMWF-ERA interim reanalysis). Heavy rain is defined as the top 5% of cases with rain, sorted by maximum reflectivity in the surroundings of the RO. The brown-shaded region shows the standard deviation for the differences from RO to GFS, while the gray shading shows the standard deviation to ECMWF-ERA. ECMWF-ERA = European Center for Medium-Range Weather Forecast; GFS = Global Forecast System; RO = radio occultation.

Juárez, M. de la T., Padullés, R., Turk, F. J. & Cardellach, E. Signatures of Heavy Precipitation on the Thermodynamics of Clouds Seen From Satellite: Changes Observed in Temperature Lapse Rates and Missed by Weather Analyses. *Journal of Geophysical Research: Atmospheres* **123**, 13,033-13,045 (2018).

Applications: Polarimetric RO Bending Angle

RO bending angle (α) data are routinely assimilated into weather forecast models

To assimilate the polarimetric $\Delta\phi$ signal, a forward operator that simulates the $\Delta\phi$ (from the model condensed water state) is required

- The RO processing extracts the bending angle at both polarizations (difference is the "polarimetric bending angle" due to precipitation)
- May offer a more straightforward way to assimilate pol-RO observations

Angle Diff (urad) Phase Diff (rad)

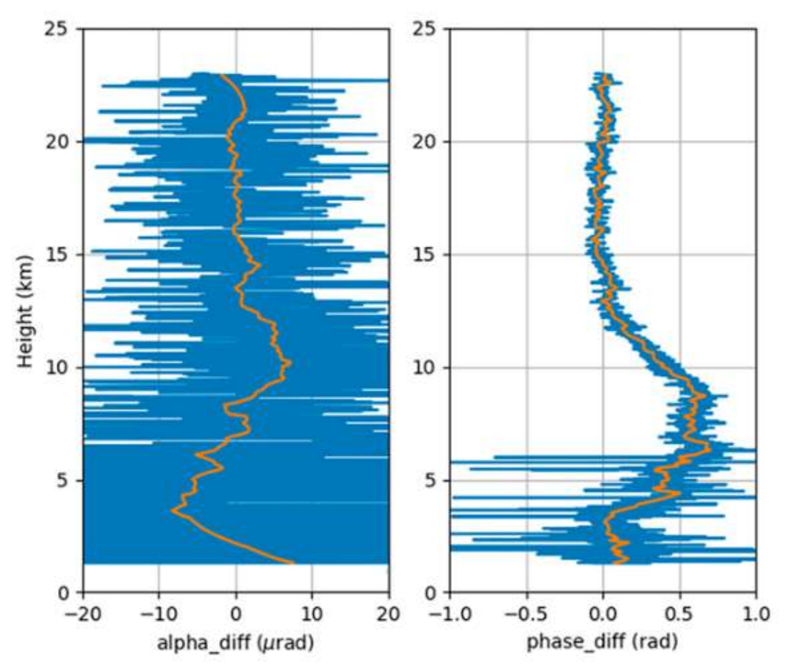

FIG. 5. The (left) bending angle and (right) phase shift between H and V channels in a case of actual *PAZ* data (20180620_0658paz_g56, 6.26 mm h^{-1}). Raw difference is shown in blue curves and the smoothed results are shown in orange curves. The shape of both curves between 4 and 12 km match the ones derived by MPS simulation.

Wang, K.-N. *et al.* The Effects of Heavy Precipitation on Polarimetric Radio Occultation (PRO) Bending Angle Observations. *J. Atmos. Oceanic Tech.*, **39**, 149–161 (2022). https://doi.org/10.1175/JTECH-D-21-0032.1

Ongoing ROM-SAF Microphysics Comparison Study
(Currently ECMWF, JMA, JPL)

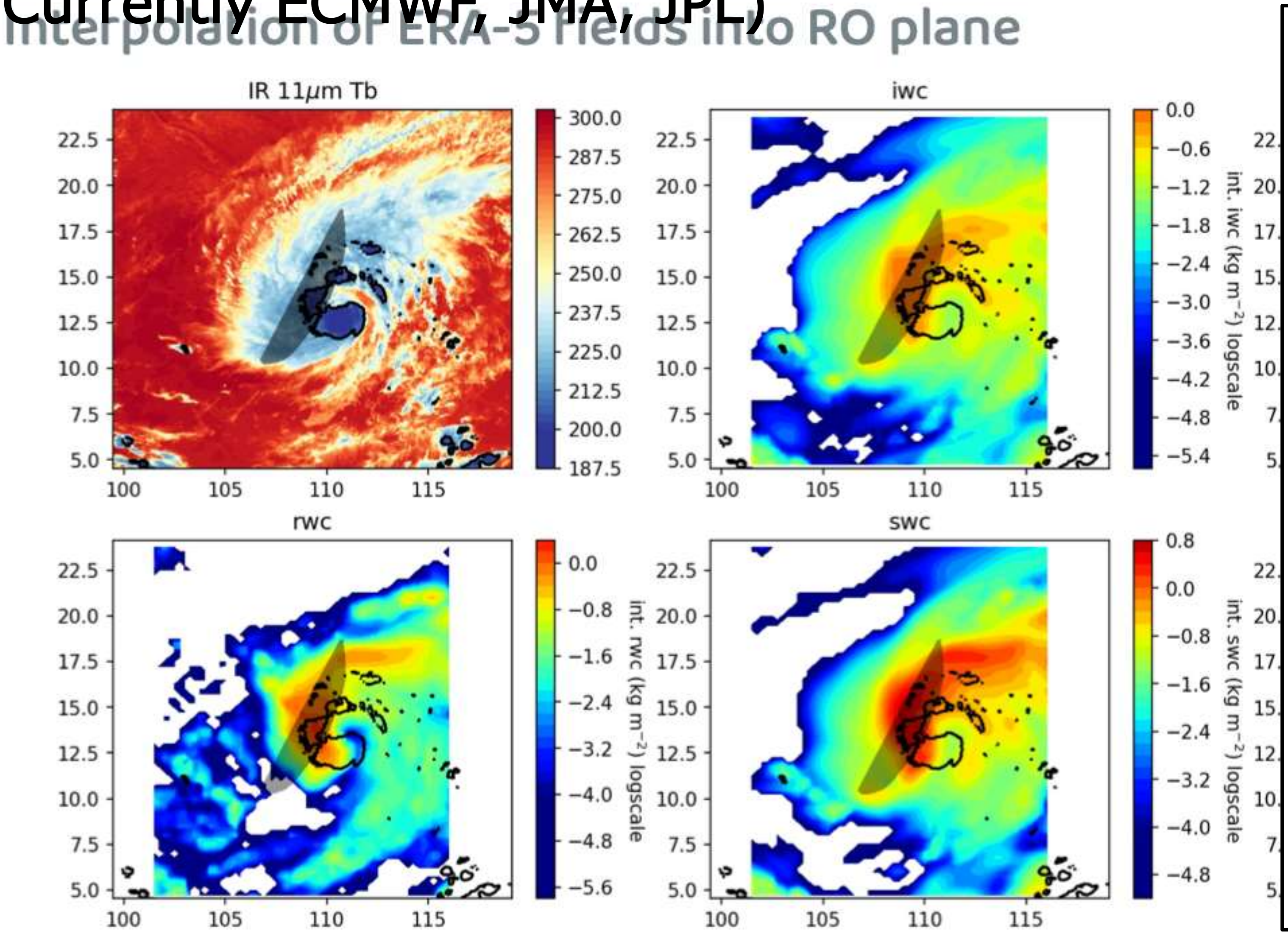

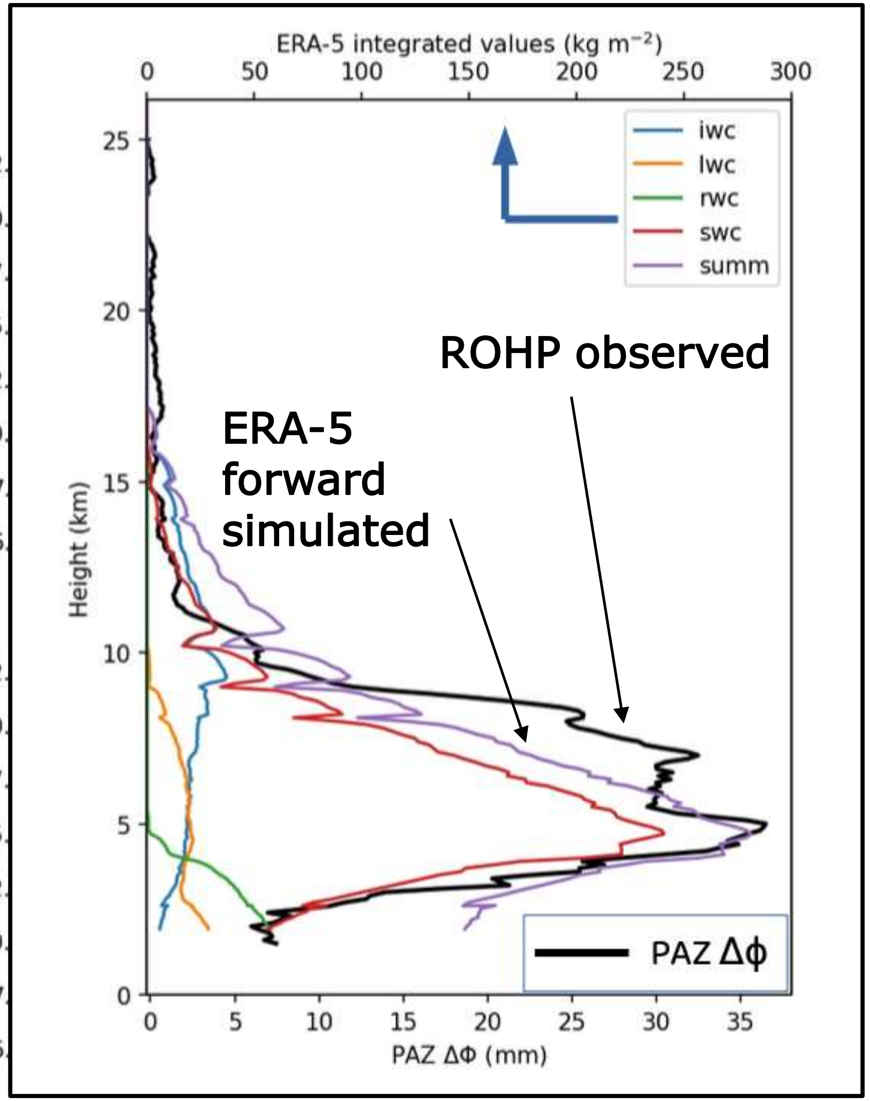

Credit: Ramon Padulles

Wrap-Up

An observational strategy (STORM-PROBE) utilizing closely-spaced polarimetric RO observations was outlined, to obtain measurements of LFT moisture within and in the environment surrounding heavy precipitation

Some other uses were described: "depth" of convection, ice water path, tropical weather, TC reconaissance, NWP applications

ROHP data (~5-yrs to date) is free and open: https://paz.ice.csic.es/

Thank you for this invitation to present

For further information, ideas, collaborations: jturk@jpl.nasa.gov

COSMIC-2 “RO Pairs”
All of 2021
Within ±10-min
< 200-km separation
Over-Ocean
±20-deg latitude

Red= e from RO-1
Orange= e from RO-2

Black= e_{sat} from RO-1
Blue= e_{sat} from RO-2

Red/Orange curves are on top of each other

Black/Blue curves are on top of each

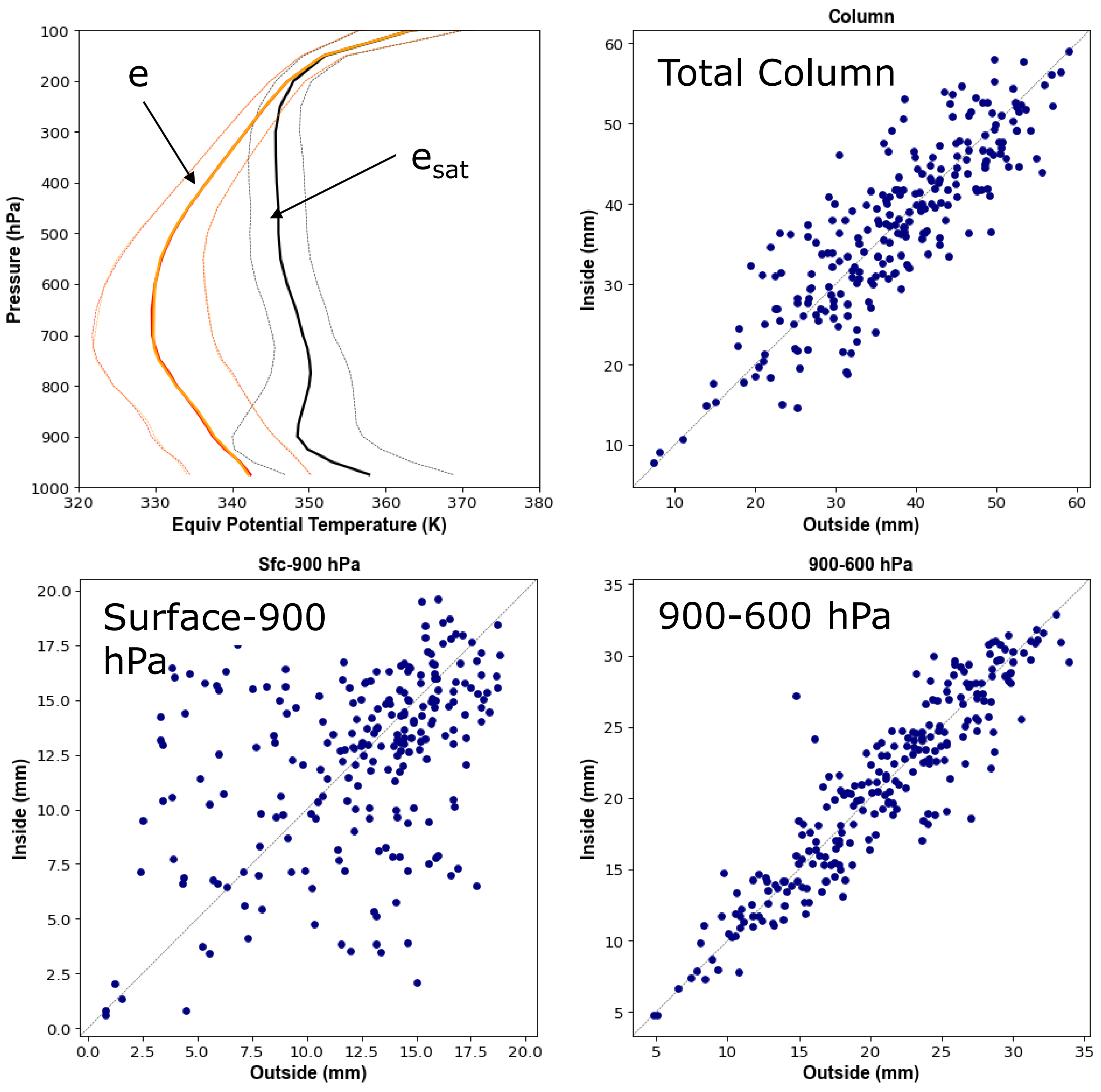

Selection Criteria:
RO-1 non-raining
RO-2 non-raining
(inferred from nearest 30-min GPM-IMERG

No discernable difference in any layer-average water vapor between RO-1 and RO-2

(sanity check)

Applications to Weather Modeling

Evaluation of the convective parameterization schemes used in climate and NWP forecast models (ROM-SAF currently study underway)

$\Delta\phi$ is a coincident, independent observation (not currently assimilated). Use $\Delta\phi$ signal to pinpoint details of model bias under heavy precipitation conditions.

Advance RO forward observation operators and the assimilation of rain-affected data.

Far-offshore reconnaissance of severe weather, tropical systems

Estimate one component of the thermal wind (set up by a change in temperature over a change in distance) (not yet investigated).

Polarimetric Radio Occultations (PRO) Concept

GNSS
RHC
transmit

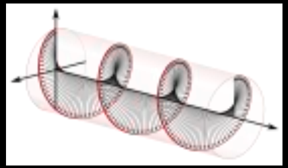

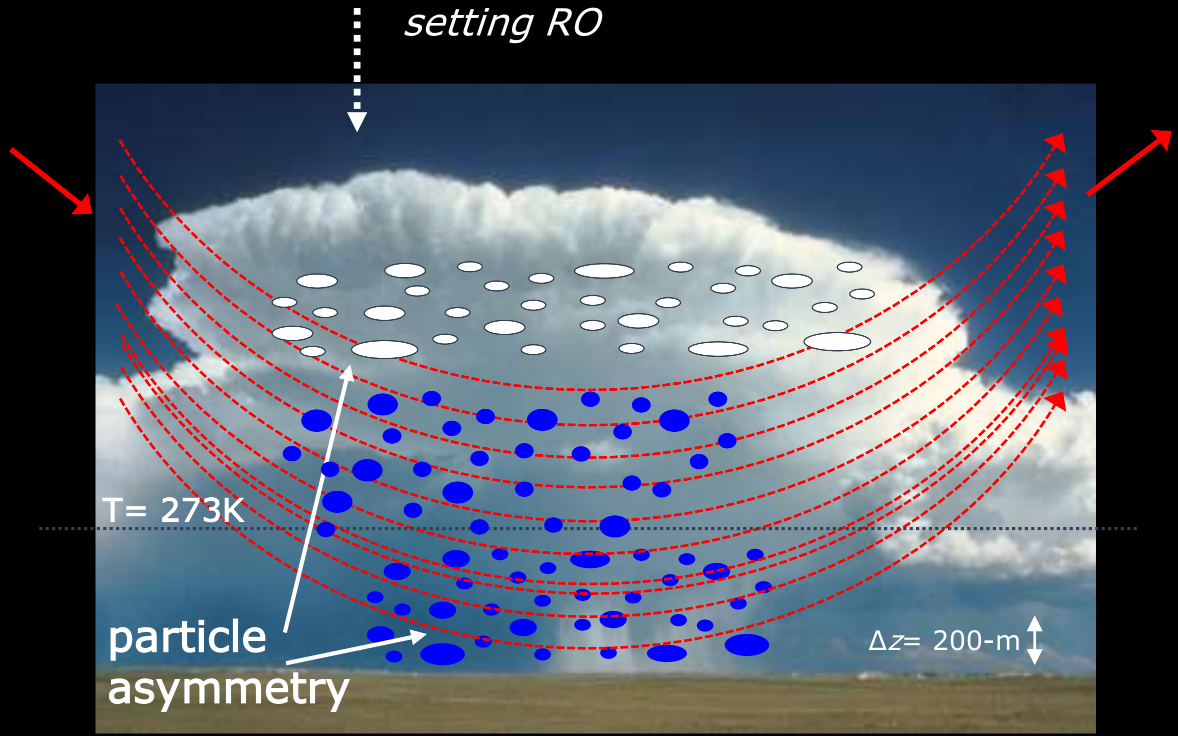

(exaggerated depiction)

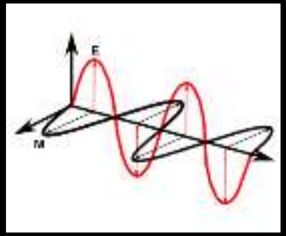

Simultaneous
H/V receive

GNSS propagation through a precipitation media induces a cross-polarized component

Measureable as a differential phase delay between H and V polarizations: $\boldsymbol{\Delta\phi}$

Extends the capability of traditional RO

$\boldsymbol{\Delta\phi}$ provides a simultaneous indication of heavy precipitation at each level

Using vertical profile information to assess convective conditions in CMIP6 models

Equivalent potential temperature (**e**) (solid lines) and saturation equivalent potential temperature (**e**$_{sat}$) (dashed lines) at the Nauru island Atmospheric Radiation Mission (ARM) site

The orange shaded area gives a measure of conditional instability for a non-entraining parcel

The gray shaded area indicates the subsaturation in the lower free troposphere (LFT) (750–900 hPa)

Two models are shown for comparison with the ARM best estimate data

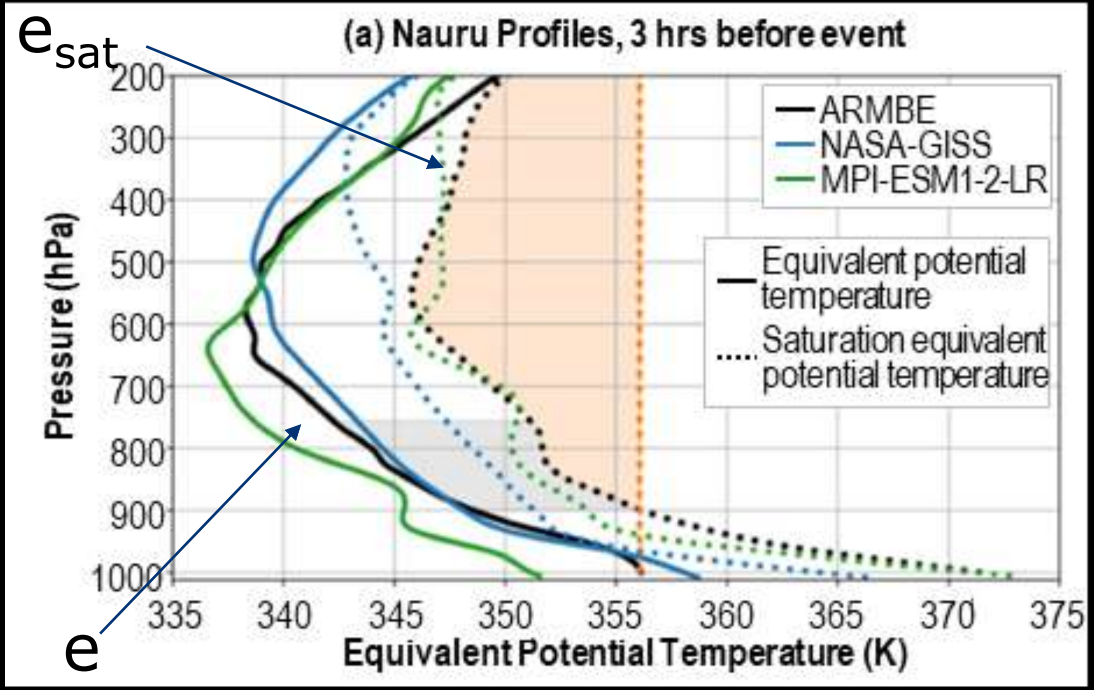

Emmenegger et. al., 2022, in review

CloudSat-TRMM and CloudSat-GPM Satellite Coincidence Data

2010/11/24 1957 (CloudSat) 2006 (TRMM) UTC

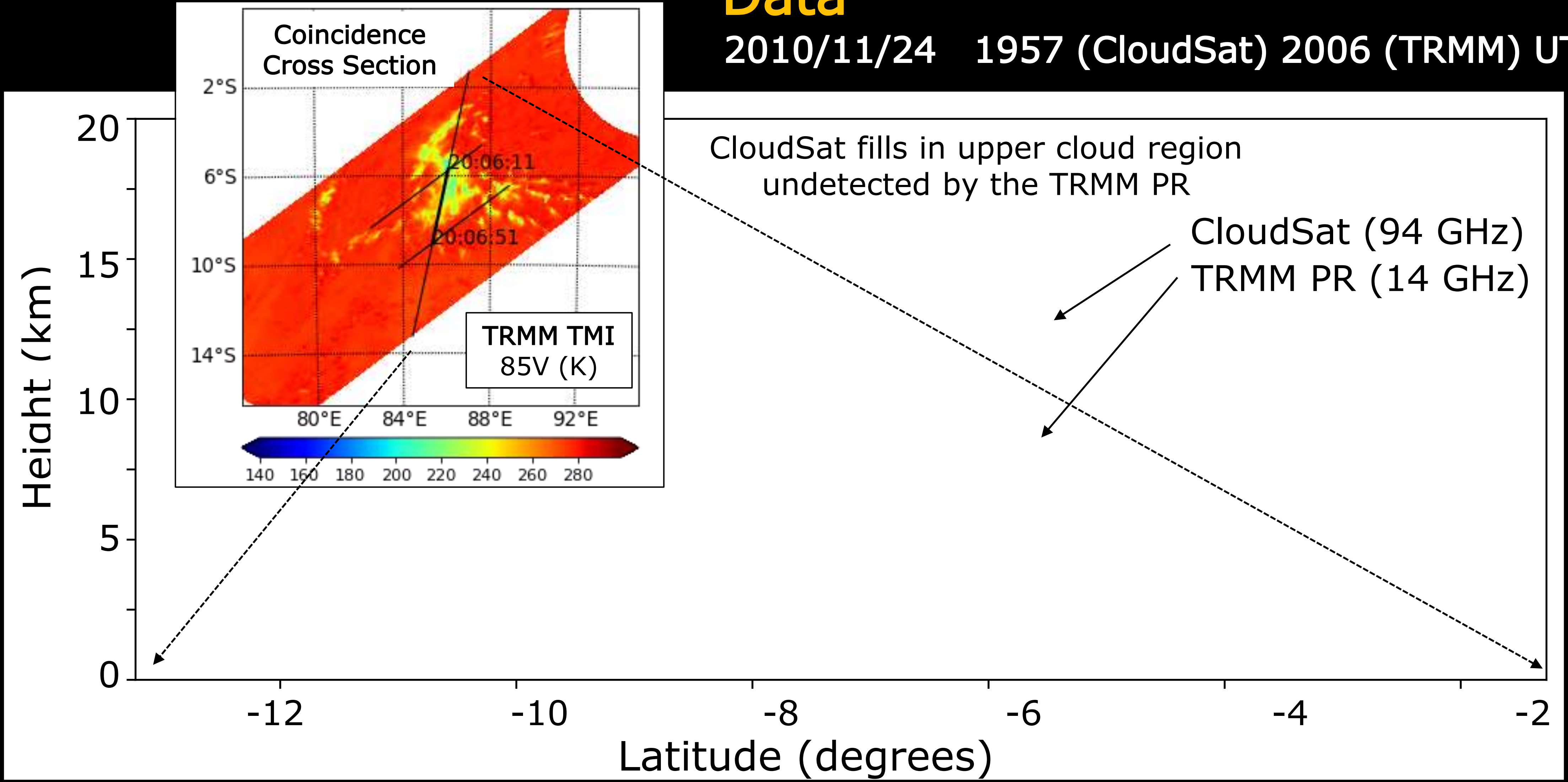

Turk, F.J., Ringerud, S.E., Camplani, A., Casella, D., Chase, R.J., Ebtehaj, A., Gong, J., Kulie, M., Liu, G., Milani, L., Panegrossi, G., Padullés, R., Rysman, J.-F., Sanò, P., Vahedizade, S., Wood, N.B., 2021. Applications of a CloudSat-TRMM and CloudSat-GPM Satellite Coincidence Dataset. https://doi.org/10.3390/rs13122264

ROHP-PAZ vertical structure of the observations

Sensing Horizontally Oriented Frozen Particles

TRMM Precipitation Radar cross section under ROHP rays

ROHP RO ray paths alongside GPM GMI 166V channel

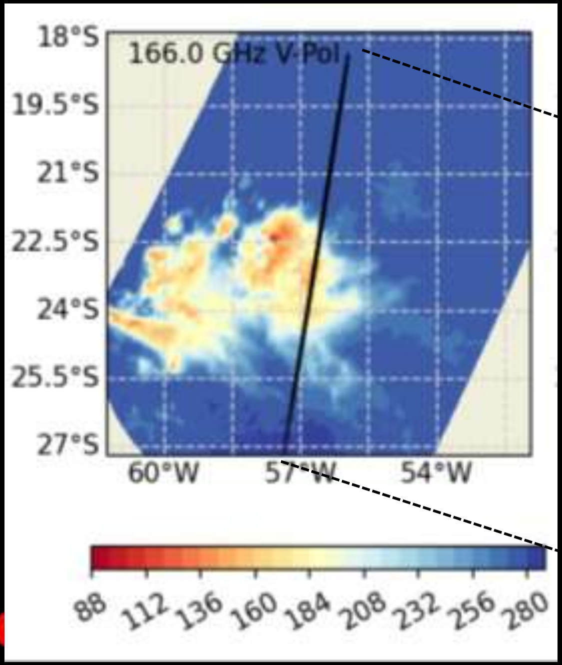

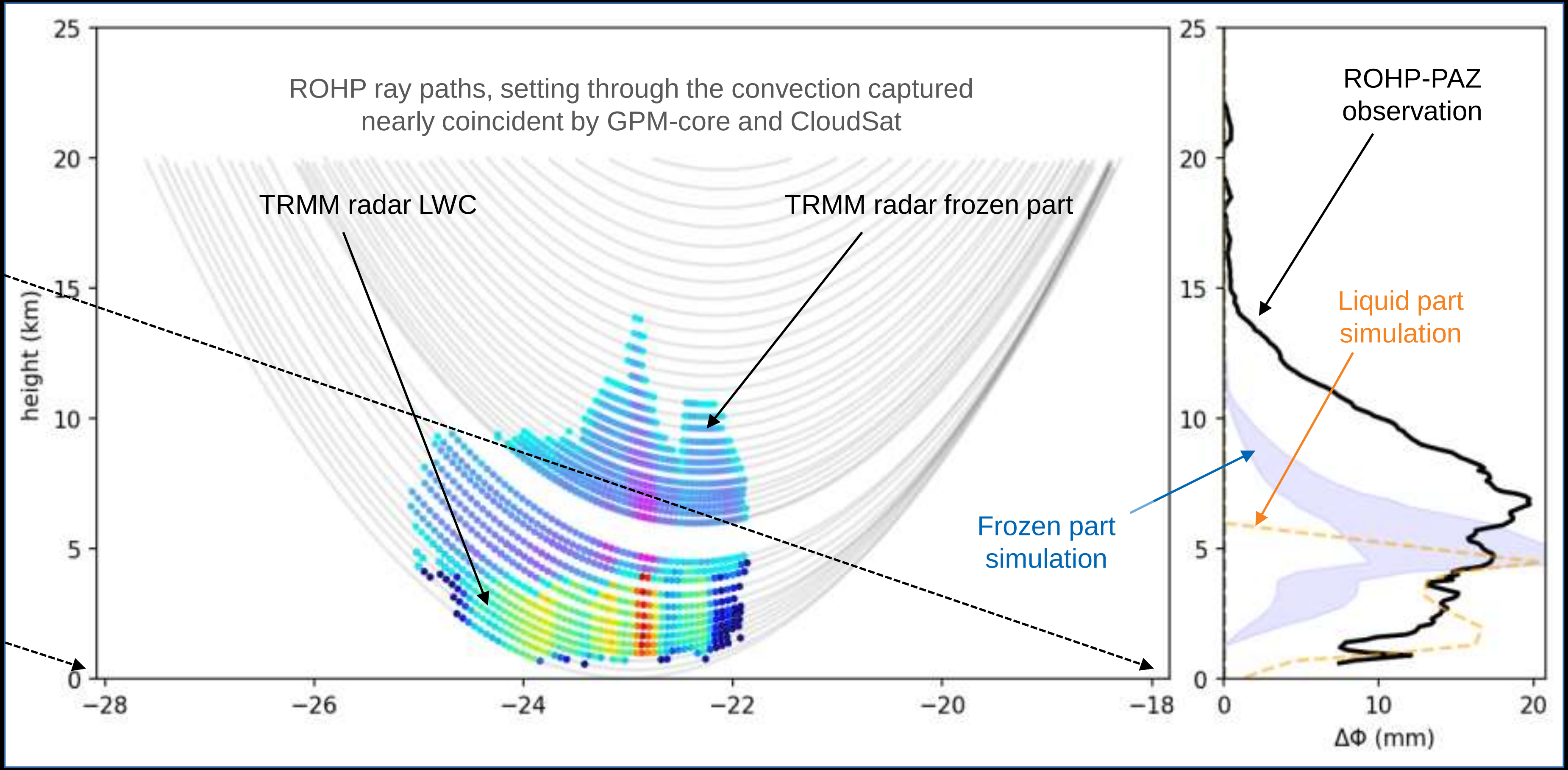

Padullés, R., Cardellach, E., Turk, F.J., Ao, C.O., Juárez, M. de la T., Gong, J., Wu, D.L., 2021. Sensing Horizontally Oriented Frozen Particles With Polarimetric Radio Occultations Aboard PAZ: Validation Using GMI Coincident Observations and Cloudsat a Priori Information., https://doi.org/10.1109/TGRS.2021.3065119

ROHP-PAZ vertical structure of the observations

Sensing Horizontally Oriented Frozen Particles

TRMM Precipitation Radar cross section under ROHP rays

ROHP RO ray paths alongside GPM GMI 166V channel

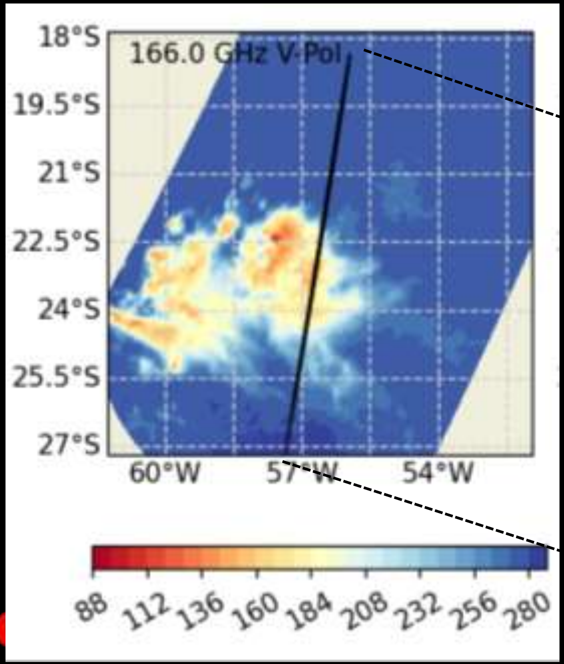

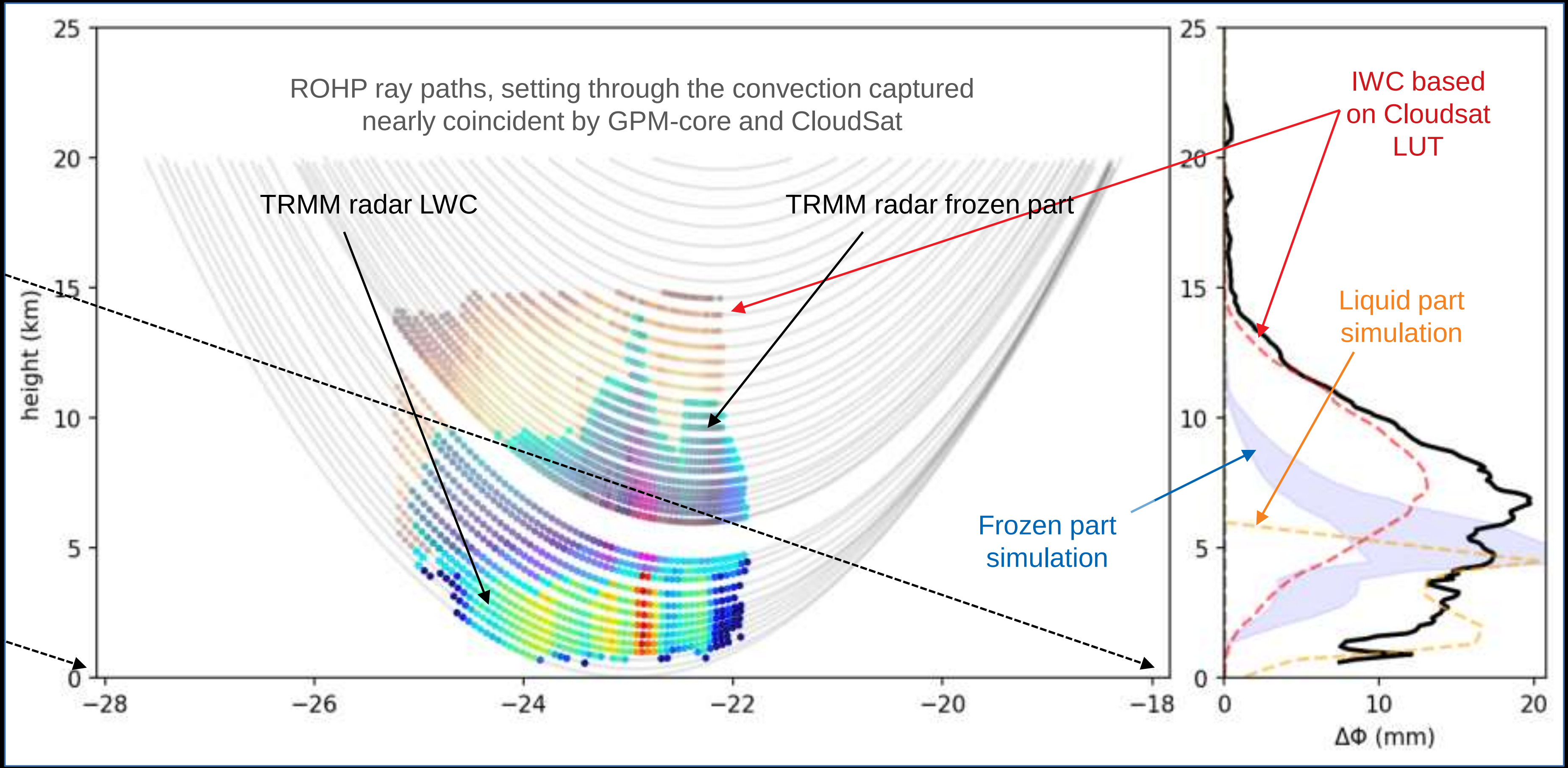

Padullés, R., Cardellach, E., Turk, F.J., Ao, C.O., Juárez, M. de la T., Gong, J., Wu, D.L., 2021. Sensing Horizontally Oriented Frozen Particles With Polarimetric Radio Occultations Aboard PAZ: Validation Using GMI Coincident Observations and Cloudsat a Priori Information., https://doi.org/10.1109/TGRS.2021.3065119

All RO Data (After Quality Control) JJA 2022

Only RO reaching to at least 920 hPa (ocean) or to within 500-m of terrain height (land)

Only COSMIC-2 data: Number per 1-degree

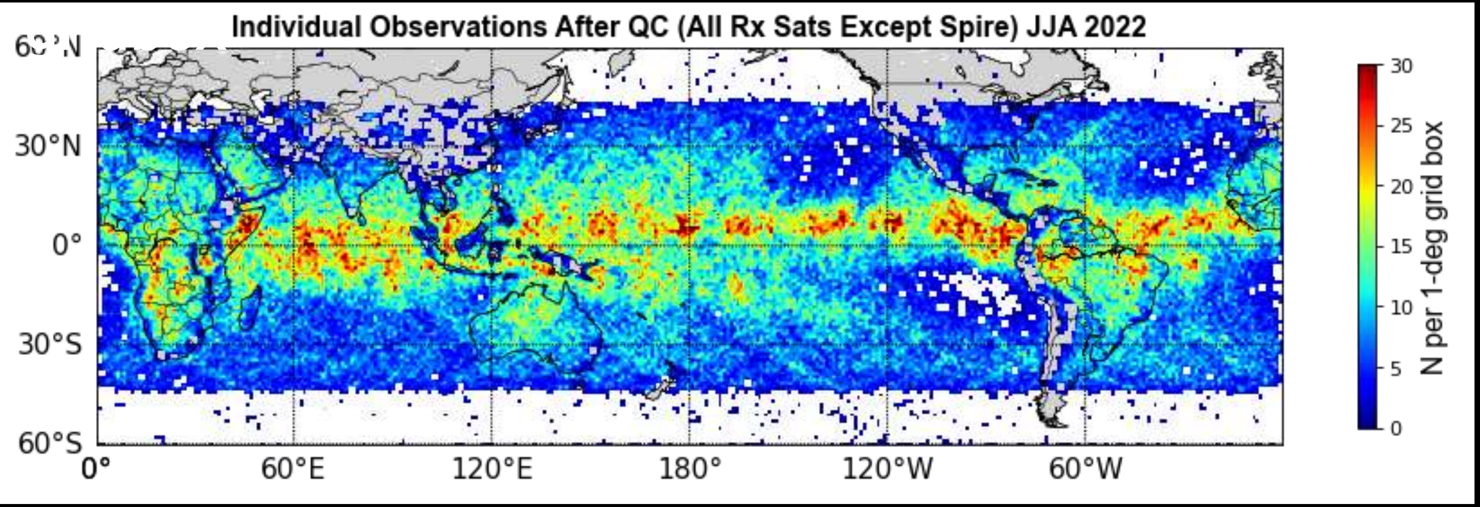

Zonal Total

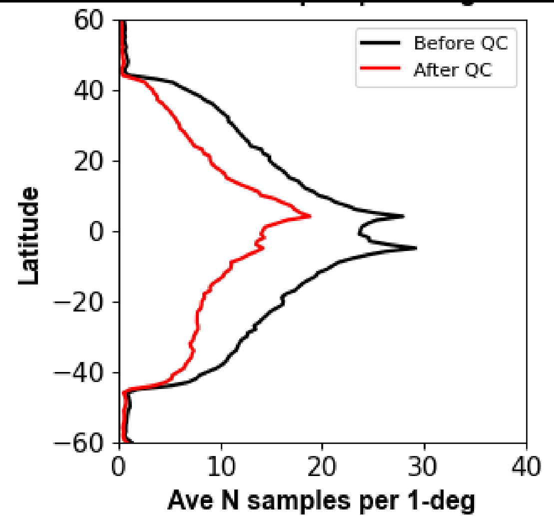

Including Spire data

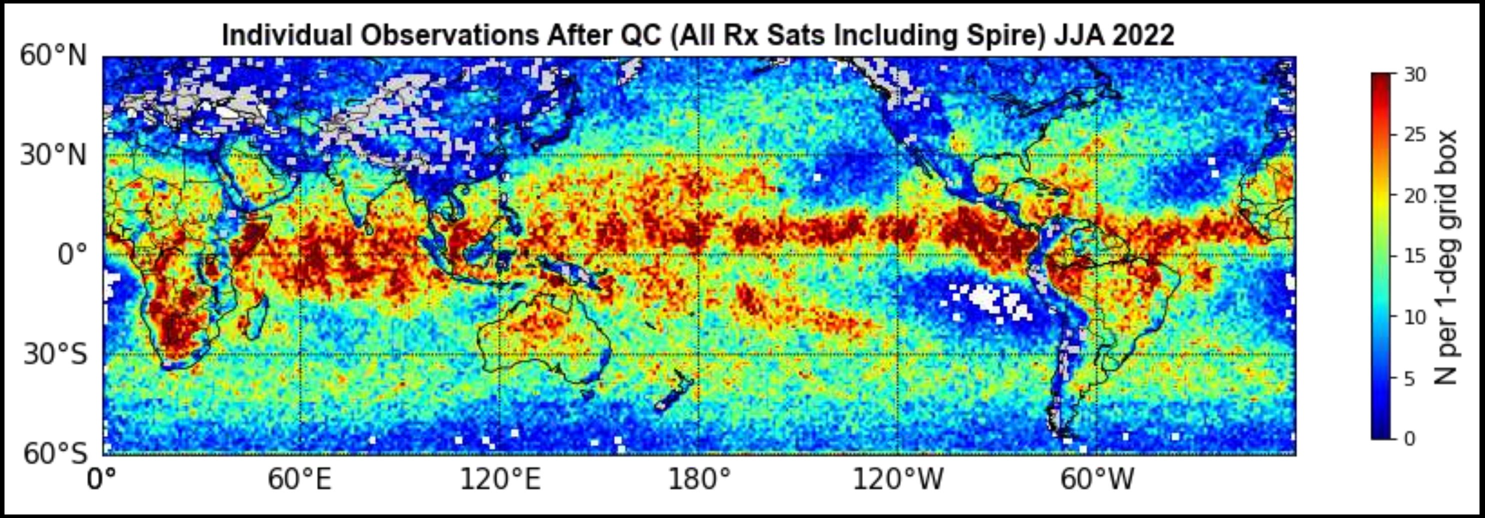

Zonal Total